

**An-Najah National University
Faculty of Graduate Studies**

**Removal of Trimethoprim from Wastewater Using
Organically Modified Silica with Pyrazole-3-
carbaldehyde Bridged to Copper Ions: Experimental
and Theoretical Approach**

**By
Elham Mohammed Said Dawod Al-sheikh**

**Supervisor
Prof. Shehdeh Jodeh**

**This Thesis is Submitted in Partial Fulfillment of the Requirements for
the Degree of Master of Chemistry, Faculty of Graduate Studies,
An-Najah National University, Nablus, Palestine.**

**Removal of trimethoprim from wastewater using organically modified
silica with pyrazole-3-carbaldehyde bridged to copper ions:
Experimental and Theoretical approach.**

By

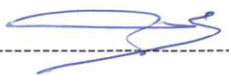
Elham Mohammed Said Dawod Al-sheikh

This thesis was defended successfully on 10/8/2021 and approved

by:

Prof. Shehdeh Jodeh (supervisor)-----

Dr. Suleiman Saleh (External Examiner)-----

Dr. Mohyeddin Assali (Internal Examiner)-----

Dedication

To my beloved husband

To my mother and father

To my brothers and sisters

To my babies

To all my friends who spare no effort to help

To all the people of Palestine

I dedicate this modest work

Acknowledgements

All thanks to Allah, the lord of the worlds and peace and blessings of Allah be upon the noblest of the Prophets and Messengers, our Prophet Mohammad.

I wish to express my great thanks to Prof. Shehdeh Jodeh, my Supervisor of this work, for all supporting and advice in my research work.

I am also most grateful to all my doctors in chemistry department in my University, An-Najah National University for all facilities they have generously provided me.

I am also grateful to all my professors (agiant in the Department of Chemistry) at An-Najah National University.

I like to thank Professor Smaail Radi and Dr. Said Tighadouin for preparing the compound in their labs at Mohammed Premier University in Morocco.

I would like to thank all the technicians and staff of the chemistry department at An-Najah National University, especially Mr. Omair Al-Nabulsi and Mr. Nafiz Dweikat for their assistance.

I like also to thank all friends in the master program for the great and lovely time that we spent together.

Finally, my thanks to everyone who helped me in my work?

أنا الموقعة أدناه، مقدمة الرسالة التي تحمل عنوان:

Removal of Trimethoprim from Wastewater Using Organically Modified Silica with Pyrazole-3-carbaldehyde Bridged to Coper Ions: Experimental and Theoretical Approach

أقر بأن ما اشتملت عليه هذه الرسالة هي نتاج جهدي الخاص، باستثناء ما تمت الإشارة إليه حيثما ورد، وأن هذه الرسالة ككل أو أي جزء منها لم يقدم من قبل لنيل أية درجة أو لقب علمي أو بحثي لدى أية مؤسسة تعليمية أو بحثية أخرى.

Declaration

The work provided in this thesis, unless otherwise referenced, is the research's own work, and has not been submitted elsewhere for any other degree or qualification.

Student's Name:

اسم الطالبة:

Signuter:

التوقيع:

Date:

التاريخ:

vi
List of Contents

Dedication	iii
Acknowledgements	iv
Chapter One: Introduction	1
1.1. Overview	2
1.2 Objectives of this work	5
1.2.1 General Objectives	5
1.2.2 Specific objectives	5
1.2.3 Research question and identified problems	6
Chapter Two: Background and Literature Review	7
2.1 Trimethoprim (TMP)	8
2.1.1 Properties of TMP	8
2.2.1 Mechanism of TMP:	9
2.3 Environmental impact of TMP:	10
2.4 Adsorption.....	12
2.4.1 Definition of Adsorption	12
2.4.2 Types of Adsorption.....	13
2.4.3 Application of adsorption.....	15
2.4.4 Adsorption as an effective method for removing TMP from wastewater	16
2.4.5 Types of adsorbents.....	17
2.4.6 Adsorption isotherms models.....	18
2.4.7 Adsorption kinetics	20
2.4.8 Adsorption Thermodynamics.....	21
2.5 Chelating material, Immobilized Ligand Systems.....	22
2.5.1 Definition of chelating material	22
2.5.2 Chelating material advantages	22
2.5.3 Preparation of a solid support matrix immobilized ligand system	23
2.6. Methodology of preparing a solid support matrix surface modified with 1,5-dimethyl-1-H-pyrazole-3-carbaldehyde	23

2.7 Computational details.....	24
2.7.1 DFT part	24
Chapter Three: Experimental Part.....	26
3.1 Chemicals and Materials	27
3.2 SiNP Synthesis:	27
3.3 Preparation of Trimethoprim solutions	28
3.4 Calibration Curve	28
3.5 Adsorption Experiments.....	29
3.5.1 Experiment (1): Optimize the contact time.....	30
3.5.2 Experiment (2): pH value effect.....	30
3.5.3 Experiment (3): Temperature effect.....	31
3.5.4 Experiment (4) Trimethoprim initial concentration effect	31
3.5.5 Experiment (5) - Adsorbent dose effect.....	31
3.6 Kinetics and Thermodynamics of Adsorption	32
Chapter Four: Result and Discussion	33
4.1 Characterization:	34
4.1.1 FT-IR Characterization	34
4.1.2 Scanning Electron Micrographs.....	35
4.1.3 TGA Analysis and Thermal Stability	36
4.2 Investigation of adsorption parameters	37
4.2.1 Contact time effect on TMP adsorption.....	37
4.2.2 pH effect on TMP adsorption.....	39
4.2.3 Temperature effect on TMP adsorption.....	41
4.2.4 TMP concentrations effects	42
4.3 Adsorption isotherm of trimethoprim	43
4.3.1 Langmuir Adsorption Isotherm.....	43
4.3.2 Freundlich Adsorption Isotherm	45
4.4. Adsorption thermodynamics	48
4.5 Adsorption kinetics of TMP.....	51
4.6 Theoretical results	55
4.6.1 DFT study.....	55

4.6.2 Monte Carlo (MC) and Molecular Dynamic (MD) simulation	59
Conclusions	64
Recommendations	66
References	67
الملخص	ب

List of Tables

Table 1: properties of TMP	9
Table 2: Pervious studies for removal of TMP from wastewater	11
Table 3: Comparison between Physisorption and Chemisorption.....	14
Table 4: Langmuir isotherm and correlation coefficient parameters of adsorption of trimethoprim on modified (Si NP)	45
Table 5: Freundlich isotherm parameters and correlation coefficient for adsorption of trimethoprim on (Si-NP).....	47
Table 6: correlation coefficient and parameters of Langmuir, Freundlich for adsorption of TMP on (Si-NP) at 308, 315. 320 K.....	48
Table 7: The thermodynamic parameters on TMP adsorption	50
Table 8: The kinetic parameter for TMP adsorption on SiNP	53
Table 9: Intraparticle diffusion model parameters	54
Table 10: Quantum global reactivity descriptors of the TMP molecule	57
Table 11: Statistics of the interaction energy of the TMP molecule onto modified silica surface during MD (energy values are in kcal/mol).	62

List of Figures

Figure 1: The structural formula for Trimethoprim	8
Figure 2: summarize OF synthetic procedure	23
Figure 3: calibration curve between absorbance vs concentration for TMP concentrations in the range 0-30 mg/	29
Figure 4: FT-IR Spectra of SiG, SiNH ₂ and SiNP	35
Figure 5: . SEM images of SiNP (A), SiNP-Cu (B)	36
Figure 6: TGA analysis of free silica (a), of SiNP (b), SiNP-Cu (c)	37
Figure 7: Effect of contact time of TMP adsorption on SiNP	39
Figure 8: pH effect on adsorption of TMP on SiNP	40
Figure 9: Temperature effect on adsorption process.....	42
Figure 10: Effect of adsorbent dose on the adsorption process	43
Figure 11: Langmuir plot for TMP adsorption on modified (SiNP).....	44
Figure 12: Freundlich plot for TMP adsorption on (Si-NP)	46
Figure 13: Adsorption thermodynamics of TMP onto SiNP	49
Figure 14: A pseudo-first order kinetic model.....	52
Figure 15: the second order kinetic model.....	53
Figure 16: : Intra particle diffusion model	54
Figure 17: (a) optimized structure, (b) HOMO, (c) LUMO and (d) molecular electrostatic.	56
Figure 18: Graphical representation of the LRDs.....	58
Figure 19 Figure 1(a) The size of the simulation box containing the modified silica surface and the vacuum layer, (b) MC pose of the lowest adsorption configurations for onto Modified silica surface and (c) Lowest energy configurations of the interaction of TMP molecule onto modified silica surface obtained by MD.	60

List of Abbreviation

Symbol	Abbreviation
AAS	Atomic absorption spectroscopy
C_o	Concentration of for TMP in the sample solution before treatment (mg/L)
C_e	Concentration of for TMP in the sample solution after treatment (mg/L) at equilibrium
C_i	Initial concentration of TMP (mg/L)
DMSO	Dimethyl Sulfoxide
EMB	Eosin Methylene Blue Agar
EDX	Energy dispersive X- ray
FT-IR	Fourier Transform Infrared
G⁽⁻⁾	Gram-negative bacteria
G⁽⁺⁾	Gram-positive bacteria
ΔG^o	Standard free Gibbs energy
ΔH^o	Standard enthalpy
K₁	The first order rate constant
K₂	The pseudo second order rate constant
K_d	The distribution coefficient
K_F	Freundlich constant which is an approximate indicator of adsorption capacity of the sorbent (mg/g (L/mg) ^{1/n})

K_L	Langmuir isotherm constant (L/mg)
min	minute
m_{sed}	Mass of adsorbent dose
n	Dimensionless Freundlich constant giving an indication of how favorable the adsorption process
OPT	Occupied Palestinian territories
PCBS	Palestinian Central Bureau of Statistics
Q_e	The capacity :TMP amount of adsorbed per gram of the adsorbent in (mg/g)
Q_m	Maximum capacity in (mg/g)
Q_t	TMP amount per unit mass of adsorbent at time t (min)
R	Gas constant (8.314 J/mol K)
R²	Correlation coefficient (regression coefficient)
R_L	Dimensionless constant separation factor
ΔS°	Standard entropy
SEM	Scanning electron microscope
Si-NH₂	3-aminopropyl-functionlized silica gel
SiNP	Organically Modified Silica with Pyrazole-3-carbaldehyde
SPE	Solid Phase Extraction
t	Time
T	The absolute temperature (K°)

TGA Thermal gravimetric analysis

**UV-
visible** ultraviolet-visible

V Volume of solution

WHO World Health Organization

Removal of Trimethoprim from Wastewater Using Organically Modified Silica with Pyrazole-3-carbaldehyde Bridged to Copper Ions: Experimental and Theoretical Approach

By

Elham Mohammed Said Dawod Al-sheikh

Supervisor

Prof. Shehdeh Jodeh

Abstract

Wastewater has recently become a source of concern due to specific toxicities and environmental pollution.

Antibiotics pose a health risk to humans. **TMP** is one of the antibiotics that found in wastewater, the main issue here is attempting to remove it by adsorption.

We will use the synthesized material of the activated silica gel with 3-aminopropyltrimethoxysilane after preparation to form the new modified sorbent SiNP. The new chelating sorbent prepared, but we work to react it with copper sulfate for bridged to copper ions, this modified material will use as a new sorbent for removal of **TMP** from wastewater. The modified surface shows good thermal stability determined by (TGA). The FTIR and UV results confirmed that 1,5-dimethyl-1H-pyrazole-3-carbaldehyde units have immobilized at the surface of the modified silica gel. SEM images of the modified Silica surface showed tough and porous nature, indicating that the materials present good characteristics to use as an adsorbent. The synthesized modified SiNP investigated as an adsorbent for removal of **TMP**. The adsorption experiments were carried for a wide range

of different solution pH, adsorbent dosage of different weights, temperature, initial concentration of solutions and contact time. The results show that the percentage removal of **TMP** increase with those mentioned parameters. Over removal efficiency of **TMP** was achieved after 100 min., at solution pH around 8 and 25 °C temperature, 0.03 g weight of dose and initial concentration of 10 mg/L **TMP** solution.

The values that obtained by pseudo second order model, are Q_e calc. 42.86, 22.23, 47.85 mgg^{-1} , were consistent with the experimental values, Q_e exp. 19.32, 20.38, 20.46 mgg^{-1} at 308, 315, 320 K, respectively, a plot was having good correlation coefficient close to 1, indicate that the adsorption can be represented by the pseudo second order model.

From Freundlich isotherm model parameters, value of $n = 1.3817$ to 1.1902 at different temperature were studies indicating that the adsorption of **TMP** on (Si-NP) is favorable. The adsorption data suited with Langmuir and Freundlich, but Freundlich adsorption model found to have the highest regression value and the best suit. The Freundlich model suggests physical adsorption and a heterogeneous distribution of active sites on the surface of the adsorbent.

The positive ΔG° values (2.933 to 2.901 kJ/mol) indicate that the adsorption is favorable and nonspontaneous at studied temperatures. The positive value of ΔH° (3.785 kJ/mol) reflects an endothermic

adsorption and indicates that the adsorption is favored, at all studied temperature. A positive value of ΔS° 2.771J/mol. K suggests that the adsorption process involves a dissociative mechanism. The adsorption leads to increase in degree of freedom during the adsorption process of TMP at different temperatures.

A positive value of ΔS° reflects that some change occurs in the internal structures of the adsorbent during the adsorption process. (Si-NP) is a good effective adsorbent for the removal of TMP from the wastewater.

Chapter One

Introduction

Chapter One

Introduction

1.1. Overview

Water pollution has become a global issue that affects all nations without exception. People becoming increasingly sick as a result, of drinking contaminated water, and nearly 14000 people die every day a result of water-related diseases [1].

Concerns about insufficient water resources have grown in recent decades, as have concerns about toxicity compounds in pharmaceutical and hospital wastewater. Medications and antibiotics pose a threat to human and animal health [2]. During the processing and use of medications, these chemicals released into the setting.

Heavy metals [3], personal care products and pharmaceuticals [4], dyes [5], agricultural by product [6], and endocrine disrupting compounds [7] are among the contaminants found in both drinking water and wastewater.

Surface water, ground water [8], streams, soil, sediment, and Sewage treatment plant effluents [9], have all found to contain antibiotics.

The antibacterial drug trimethoprim (**TMP**) together with the sulfonamide (sulfamethoxazole) commonly used in the treatment of bacterial infections. The antibacterial action inhibits folic acid synthesis, which decreases the risk of bacteria developing resistance.

The most commonly found pharmaceuticals in wastewater are sulfamethoxazole (SMX) and Trimethoprim (TMP) [10]. In wastewater effluent, these compounds found at levels of 2-1830ng/L and 308-791ng/L, respectively after secondary treatment [11]. Wastewater treatment plant influents, hospital effluent and livestock effluent are the major sources of TMP in wastewater. Because of the high use of livestock effluent, it had a very high SMX/TMP ratio [12].

Antibiotics must be removed from water sources due to negative effects such as bacteria producing a resistant gene [2]. There are a variety of water remediation technologies available: membrane filtration [14], electrodialysis [15], oxidation, [16], ozonation [17], ion exchange [18], electrochemical [19], reverse osmosis [20], evaporation, distillation, sedimentation, crystallization, flotation, centrifugation, coagulation and adsorption [21]. Municipal wastewater treatment plants (WWTPs) are unable to remove organic micro pollutants that escape treatment in WWTPs [22]. **TMP** is not easily removed by traditional wastewater treatment systems. The quest for a low-cost, readily available adsorbent has more economic techniques, and is a promising and widely used tool.

Solid-Phase Extraction (SPE) is a technique for the isolating of pollutants from water that has shown to be effective in water treatment. This technology has a number of significant advantages including: (i) Analyte recovery is high, and there is no emulsion (ii)

automation ease (iii) safety, versatility and simplicity,(iv) high selectivity and sensitivity, (v) low cost and fast, (vi) Because of its ability to combine with a variety of modern detection techniques. This hybrid extraction or clean up approach has reduced sample handling time. (vii) the capacity to extract analgesics at the same time. SPE's flexibility allows it to use for a variety of tasks, including purification, desalting, and trace enrichment [23].

One of the most effective adsorbents is chemically modified chelating material. Modifications made to the polar adsorption content. Because of its thermal stability and mechanical strength, silica gel has used as an inorganic stable matrix in inorganic-organic materials. The surface of the silica particle is heterogeneous, with a number of different types of silanol groups present, and the presence of active donor atoms in the incorporated organic moieties may modify surface properties, the surface usually modified by bonding a wide variety of functional groups to the surface. Chemical modification of the skeleton of silica gel made covalent coupling of an organic moiety to obtain good adsorbents [24]. The mechanism is depending on the charged function group in the compound attracting the charged group bonded to the silica surface through electrostatic attraction. Modified Silica with pyrazole-3-carbaldehyde bond with copper ions can be synthesized and characterized as a new sorbent with a porous but rigid content with a high surface area. The chemical and thermal stability of this substance is excellent [25-26].

The aim of this study is to remove **TMP** from wastewater, using this prepared of SiNP -Cu in the solid-phase extraction method. The adsorption behaviors of the adsorbent with **TMP** will studied. The effect of pH, temperature, and amount of adsorbent, concentration and the contact time on the adsorption of **TMP** kinetics and pH effects. Equilibrium isotherm studies will have done by varying the following three parameters: initial concentration of **TMP** solution, volume of the **TMP** solution, and adsorbent dose on the uptake of **TMP** from the solution.

1.2 Objectives of this work

1.2.1 General Objectives

1. To prepare a modified silica with pyrazole-3-carbaldehyde bond with copper ions as sorbent for **TMP**.
2. To characterize modified silica (SiNP) bond with copper ions.
3. To specify the optimal conditions for the adsorption.
4. To recover **TMP** and reuse the adsorbent.

1.2.2 Specific objectives

1. To determine if (SiNP) bond with copper ions can used to clean up **TMP** polluted wastewater.
2. To determine the extent that modified silica gel compound can tolerate and adsorb **TMP**

3. To study the effect of pH, temperature, amount of adsorbent, concentration and contact time on the adsorption of **TMP**

1.2.3 Research question and identified problems

The main questions addressed in this thesis are:

1. Can (SiNP) bond with copper ions used to clean up **TMP** polluted wastewater.
2. To which extent that (SiNP) bond with copper ions can tolerate and adsorb **TMP**?
3. What are the optimum condition of pH, temperature, amount of adsorbent, concentration, and contact time for (SiNP) bond with copper ions to adsorb **TMP** efficiently?
4. What is the adsorption behavior of the adsorbent with **TMP**?

Chapter Two

Background and Literature Review

Chapter Two

Background and Literature Review

2.1 Trimethoprim (TMP)

2.1.1 Properties of TMP

Trimethoprim (**TMP**), ($C_{14}H_{18}N_4O_3$):5-(3,4,5-Trimethoxybenzyl) pyrimidine-2,4- diamine. The structural formula is showed below [10]:

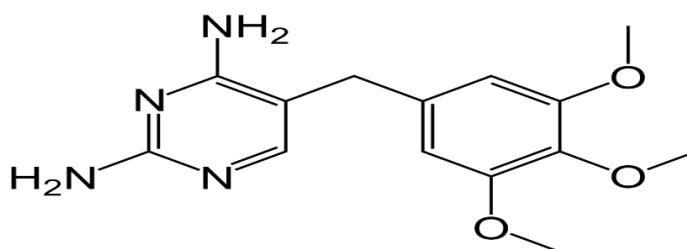


Figure 1: The structural formula for Trimethoprim

TMP is a weak base that has a pKa of 7.4. The color of white with crystalline powder that has odorless and bitter compound. **TMP** has slightly solubility in chloroform including ethanol and acetone while it is almost insoluble in water with high solubility in glacial acetic acid solution.

TMP can bond with metal ions to form **TMP** metal complexes, when the nitrogen of the pyrimidinyl ring reacts with the transition metal ions, and it used as a corrosion inhibitor. The complexes are octahedral in shape and have electrolyte properties.

The Properties of **TMP** summarized in Table 1:

Table 1: properties of TMP

Origin of the name	Derived from trimethoxy-pyrimidine
Molecular weight	290.32g/ molL
pKa	7.4
Solubility	DMSO: soluble
Formal charge	0
State at 20°C	Solid
Melting point	199-203C
Density (g cm⁻³)	1,1648
Synonyms	Proloprim , Trimplex , Trimetoprim
Discovery date	First used in 1962
Stability	Very stable and incompatible with very strong oxidizing agents.

2.2.1 Mechanism of **TMP**:

TMP inhibits bacterial nucleic acid and protein synthesis, and it is a dihydrofolate inhibitor since it inhibits the action of dihydrofolate reductase, which converts dihydrofolate to tetrahydrofolate in bacteria. Tetrahydrofolate needed for the synthesis of purines, which are required for the development of DNA and proteins [27].

TMX inhibits the bacterial enzyme dihydrofolate reductase, resulting in the active form of folic acid, tetrahydrofolic acid THF, which is required for the synthesis of thymidine, purines, and bacterial DNA. When sulfamethoxazole and **TMP** used together, they bind to bacterial dihydrofolate reductase, preventing the formation of THF, and thus block

two steps in bacterial biosynthesis, making them bactericidal. The effectiveness of antibiotics can improve by reducing the production of resistance in combination products.

2.3 Environmental impact of TMP:

TMP is one of the most antibiotics that is used around the world and usually found in the environment and affecting both surface water, ground water and soil. Antibiotics are widely used because of their efficiency and low cost, but when they excreted from individuals into wastewater or water bodies, they have negative consequences, such as the development of bacteria with antibiotic resistance genes [28]. In aquatic environments, 1 mg/L **TMP** would be a generally safe exposure limit.

The toxicity of two antimicrobial medicines (oxytetracycline and **TMP**) in the aquatic environment studied and found to be low. However, studies have found that combining **TMP** with sulfamethoxazole doubles the risk of miscarriage in early pregnancy.

The investigations found that roughly 1mg/L acts as a safe exposure limit in aquatic environments when determining the concentration of **TMP** for resistance. The highest concentration seen in untreated municipal wastewater is (0.17 mg/L-8.8 mg/L). As a result, it critical to halt the spread of antibiotic resistance.

As a result, antibiotics must remove from water sources. **TMP** removal from wastewater has studied in a number of municipal wastewater treatment plants. **TMP** not adequately removed by conventional

wastewater treatment processes. Any technique that enhances the quality of water to make it suitable for a certain end-use known as water treatment.

Physical, chemical, and biological processes are all examples of processes.

Wastewater treatment and recycling technologies coupled for safe drinking water using low-cost and appropriate technology. The technologies used for three purposes [29]:

1. Primary treated water by several techniques like filtration and centrifugal separation and flotation are examples of fundamental water treatment technologies.
2. Secondary treatment water, which involves aerobic process and Anaerobic Process.
3. Tertiary treatment water like distillation and evaporation, solvent extraction and other techniques including reverse osmosis.

The functionalized silica used in this work presents high affinity for the effective adsorption for TMP. There are others material used for adsorption of TMP reported in table 2.

Table 2: Pervious studies for removal of TMP from wastewater

Other methods for analysis TMP	Method	Recoveries	Ref.
Removal (the green alga <i>Nannochloris</i> sp)	HPLC-UV	-	[11]
Combining electro-Fenton and activated sludge	HPLC	89%	[79]
MSPE(Fe ₃ O ₄ @SiO ₂ /PVA-TEOS nanofiber)	UV-Vis	98.2%	[77]
Photocatalytic (S-TiO ₂ and Ru/WO ₃ /ZrO ₂ /reusable fixed plates)	LC/MS	88.6%	[80]
sewage sludge and fish waste derived adsorbents / pyrolyzed at 950C	MS , HPLC	90% , 10%	[10]

Other methods for analysis TMP	Method	Recoveries	Ref.
The biodegradation mechanism	UPLC/MS/MS /ITMS/ESI	90%	[78]
Fenton, Fe(II)-activated persulfate processes	HPLC	43.8%, 92,5%	[13]
Aluminum pillared K10 and KSF for adsorption	UV-Vis	-	[76]
Pyrazol-3-carbaldehyde –Cu ⁺² /SPE	SPE/UV-Vis	94%	<i>This work</i>

2.4 Adsorption

2.4.1 Definition of Adsorption

Heinrich Kayser, a German scientist, created the term "adsorption" in 1881. (1853-1940). Adsorption is the attraction of adsorbate molecules to an adsorbent surface caused by molecular forces such as permanent dipole, induced dipole, and quadrupole electrostatic effects, in which the repulsive and attractive forces between the sorbate and the adsorbent become balanced.

Physisorption and chemisorption are two types of adsorption. The adsorption process of a fluid phase on the surface of a liquid or a solid, results in the increasing in the concentration of a particular component, which is increase as the size of the interfacial area increase. As a result, all adsorbents have large specific surface areas and highly porous or very tiny particles.

Adsorbent refers to the solid material that supplies the adsorption surface, whereas adsorbate refers to the species that will adsorbed. Desorption is the opposite of absorption. Adsorption is one of the

most essential technologies because of its high removal efficiency, simplicity, cheap cost, environmental friendliness, and ease of maintenance. It uses a variety of adsorbents including activated carbon, biochar, metal oxide, graphene oxide, and mesoporous materials. Adsorption capacity and surface reactivity both enhanced by a large surface area.

Three steps make up the entire adsorption process. Film diffusion (external diffusion) ii). Diffusion of pores or intra particle diffusion (internal diffusion) iii). Adsorbent surface reaction to fix the adsorbate in the adsorbent's surface pores (adsorption on active sites) [30].

2.4.2 Types of Adsorption

Adsorption can be categorized into two forms based on the nature of the forces that exist between the adsorbate molecules and the adsorbent:

1. Physical adsorption (Physisorption): the adsorbate and adsorbent have a very weak attraction, which can be electrostatic, hydrogen bonds, Vander Waals, or dipole-dipole. Physical adsorption of a gas or vapor is normally liberation about 10 to 40 kJmol^{-1} of heat as the heats of liquefaction of gases or the condensation of vapors and the deviations from ideal gas behavior. If no electron exchange occurs, the adsorption energies are low, ranging from 5 to 40 kJ/mol , and adsorption is conceivable, the process is reversible, and

multilayer adsorption is conceivable. It known as Vander Waal's adsorption. Because a spontaneous process occurs, this sort of adsorption is an exothermic process.

2. Chemical adsorption (chemisorption): Chemical adsorption occurs when the force of attraction between the adsorbate and the adsorbent is nearly equal to the strength of chemical bonds, and the interactions mostly based on ionic or covalent bonds. Langmuir adsorption is another name for it. The force of attraction is very strong in chemisorption; adsorption involves electron transfer and is of high energy, ranging from 40 to 800 KJ/mol, adsorption is difficult; thus, adsorption cannot have reversed easily, and only a monolayer detected. [31].

Table 3: Comparison between Physisorption and Chemisorption

#	Physisorption	Chemisorption
1	Always exothermic with low heat of adsorption that is 20-40 kJ mol ⁻¹ . The energy usually smaller than condensation energy.	The heat of adsorption between 40-400 kJ mol ⁻¹ with the same energy in chemical reaction.
2	It has Van der Waals forces of attraction.	Chemical bond of attraction
3	It occurs at low temperature	Usually high temperature
4	Reversible process	Irreversible process
5	It describes the ease of liquefaction of the gas	Does not related to liquefaction of the gas
6	A relatively low degree of specificity.	It is highly specific
7	Occurs as a multilayers	It forms monomolecular layers
8	No need for activation energy	needs activation energy

2.4.3 Application of adsorption

The adsorption method is widely used in industry, laboratories, and a variety of other scientific processes. For the adsorption of wastewater, a number of alternative adsorbents have synthesized. The following are some of the most significant adsorption applications:

1. Enabled charcoals made from agricultural waste used in water and gas purification, metal extraction, gas mask air filters, and other applications.
2. The ability of activated carbons to eliminate colored compounds, as well as the bleaching of vegetable oils to produce a lighter color oil that is more attractive and easier to use.
3. Water Adsorption (Dehydration) and Gas Purification: Adsorbents such as zeolite, Silica gel, and Alumina are used to prevent condensable water from entering a gas processing plant prior to purification.
4. Fabric dyeing: dyes derived from natural plant or animal sources, and a considerable amount of dye was wasted; the adsorption method offers an appealing alternative to colorless wastewater decolorization.
5. Heterogeneous Catalysis: Heterogeneous catalysis is critical for all aspects of environmental chemistry since it allows different organisms to activate. With heterogeneous catalysis, lower ammonia energy costs could have achieved. Platinum used as a

co-catalyst in the hydrogen evolution reaction and can be substituted with less expensive metals such as Ni and Co.

6. Ion-Exchange Resins: ion –exchange resins with groups like –COOH, –SO₃H or –NH₂ have the ability to selectively adsorption of ions from solution. These resins commonly used in water softening and water purification.
7. Chromatography: Paper chromatography, gas chromatography, and vapor phase chromatography, as well as high-performance liquid chromatography, are all examples of chromatographic processes. For several separation methods, technology has advanced rapidly.
8. Adsorption used in the pharmaceutical industry to extend neurological tolerance to particular medications.

2.4.4 Adsorption as an effective method for removing TMP from wastewater

Several methods for removal of antibiotics from wastewater like oxidation and degradation. The limitation of some methods is usually has to do with high cost and toxicity. The advanced oxidation method is usually strong for the removal of TMP in traditional wastewater plants. Adsorption is one of the methods that is able to remove these pollutants with acceptable results. The advantages of using adsorption are simplicity, low cost, and ease of automation. One of the technique like solid phase extraction (SPE) is commonly used for separating analytes from a liquid matrix and

then purified extracts before using a chromatographic. The SPE showed several advantages like high analytes concentration with highly purified extracts and this for solutions with different polarities [32-34] .

Silica(SiO_2) can be used as a very successful adsorbing agent, it has been widely used for application in the water remediation due to good mechanical strength, undergo heat treatment cost-effectiveness, environmental friendliness, high acid resistance and easy modification. Silica can be used as an SPE sorbent without modification to increase its applicability modified by functional groups such as C_{18} , NH_2 , ionic or mixed-mode. The bond silica with polar functional groups can used to adsorb polar compounds from nonpolar matrices. The polar adsorption material is modified silica gel with free hydroxyl group on the surface. It may use to adsorb polar compounds from nonpolar matrices. Ion exchange SPE can be used for anionic compounds isolation on amino group that are bonded to silica surface and cationic compounds can be isolated with sulfonic acid groups that are bonded to the surface. The mechanism is depend on the electrostatic attraction between the sorbent and the sorbate [35-37].

2.4.5 Types of adsorbents

Natural adsorbents and synthetic adsorbents are two different forms of adsorbents. All examples of natural and synthetic adsorbents.

These materials are, cheap, abundant, and have ability for enhancement of adsorption capabilities. Each adsorbent has a different porosity, pore structure, and adsorbing surface composition.

2.4.6 Adsorption isotherms models

Adsorption isotherm is the amount of solute adsorbed per unit weight of adsorbent when the equilibrium concentration reached at constant temperature. The most common adsorption isotherms used to characterize experimental adsorption data are Langmuir and Freundlich isotherms. Both model can perfectly fit most of the adsorption experimental data trend [38]. The Langmuir isotherm is an analytical model that describes the equilibrium distribution and based on the theoretical concept that only a finite number of definite localized sites exist on an adsorbent.

The Langmuir-type isotherm based on the following assumptions: monolayer adsorption, no subsequent interactions or steric hindrances, physical forces drive binding, and all sites have the same affinity for the sorbate. For practical purposes, it is still the most commonly used Equation (2-1) can be used to calculate the Langmuir isotherm for pure component adsorption:

$$\frac{C_e}{q_e} = \frac{1}{q_m} C_e + \frac{1}{q_m K_L} \quad (2-1)$$

C_e is the adsorbate equilibrium concentration in (mg/L). q_e is the amount of **TMP** adsorbed per gram of the adsorbent in (mg/g).

q_m is maximum capacity in (mg/g). K_L = Langmuir isotherm constant in (L/mg), related to adsorption capacity (mg g^{-1}), which can be associated with the variance of the suitable area and porosity of the adsorbent, implying that a larger surface area and pore volume would result in a higher adsorption capacity.

A plotting C_e/q_e versus C_e . The parameters will calculate from the slope and intercept.

Separation factor (R_L) is a dimensionless constant. It shown in equation (2-2):

$$R_L = \frac{1}{(1 + K_L C_o)} \quad (2-2)$$

C_o is the highest initial concentration of adsorbate in (mg/L), K_L is Langmuir constant in (L/mg).

R_L is a dimensionless constant separation factor, indicate the isotherm is unfavorable if ($R_L > 1$), linear ($R_L = 1$), favorable ($0 < R_L < 1$), or irreversible ($R_L = 0$) [39].

The Freundlich adsorption isotherm is a model assumes the reactive sites above the adsorbate are distributed exponentially with the adsorption process's heat. The Freundlich isotherm model describe the removal of pollutants from the solution to a solid surface. The Freundlich isotherm assumes that the adsorption process on heterogonous surfaces have adsorption energies. Freundlich adsorption isotherm study the amounts adsorbed per unit mass of

adsorbent, Q_e , and the concentration of the pollutant at equilibrium, C_e . For Freundlich isotherm can be presented by linear form of logarithmic equation is (2-3):

$$\ln Q_e = \frac{1}{n} \ln C_e + \ln K_F \quad (2-3)$$

K_F represents Freundlich constant which express the adsorption capacity. n is the adsorption intensity. $1/n$ represents the adsorption intensity which is related to the relative distribution of the energy and usually the heterogeneity of the adsorption. A plot of $\log (C_e)$ vs. $\log (Q_e)$. From the intercept and the slope, we can calculate the parameters, K_F, n [40].

2.4.7 Adsorption kinetics

The study of adsorption kinetics is important because it reveals important information about the procedures that have been used. The mechanism of the adsorption processes explained using several kinetics models. The simple form of pseudo-first order equation is represented by Lagergren's equation (2-4):

$$\log(q_e - q_t) = \log q_e - \left(\frac{K_1}{2.303}\right)t \quad (2-4)$$

Q_e represents the amount of polluted adsorbed at equilibrium (mg/g), q_t is the amount of pollutant removed at any time (mg/g) and K_1 is the first order rate constant.

On the other hand, the pseudo-second order equation can be presented in (2-5):

$$\frac{t}{q_t} = \frac{1}{q_e} t + \frac{1}{K_2 q_e^2} \quad (2-5)$$

K_2 is the pseudo-second order rate constant (g/mg. min).

From the plots. The correlation coefficient (R^2) value shows that which model can represent the data [41].

2.4.8 Adsorption Thermodynamics

To determine whether an adsorption process is spontaneous or not, thermodynamic considerations are required. The Gibb's free energy change, ΔG° , represents the spontaneity of a chemical reaction. Both enthalpy (ΔH°) and entropy (ΔS°) coefficients are necessary to determine the Gibb's free energy of the process. Negative ΔG° occur spontaneously at a given temperature. The equation to find free energy using Eq. (2-6):

$$\Delta G^\circ = -RT \ln K_D \quad (2-6)$$

Where, ΔG° is the Gibb's free energy change (kJ. mol^{-1}), R is the ideal gas constant and T is temperature (K°) and K_D is the single point or linear sorption distribution coefficient (L g^{-1}).

The Gibbs free energy is the enthalpy (ΔH°) minus the entropy (ΔS°) multiplied by the temperature. The thermochemical parameters ΔH° and ΔS° , can be determined using Van't Hoff's plot, according to Equation (2-7) [42]

$$\ln K_d = -\frac{\Delta H}{RT} + \frac{\Delta S}{R} \quad (2-7)$$

2.5 Chelating material, Immobilized Ligand Systems

2.5.1 Definition of chelating material

Chelating resins are one of many solid adsorbents that are becoming more common due to their high adsorption capacities and selectivity. Composite chelating products silica gel have a strong mix of chelating agent and inorganic matrix particles. Silica gel can be used as a good adsorbing agent, the surface of silica particles is heterogeneous with different silanol groups. The surface of the silica material modified by using non-Polar, polar, ionic, or mixed-mode functional group to the surface.

Silica gel is an amorphous and porous type of silicon dioxide (SiO_2) that is present as sand in the environmental, alkali silicate solution used to make a wet silica gel. The hydroxyl (OH) group in the surface of silica gel can be functionalized to make a chelating group, such as polyamine. Polyamine can be covalently bond on the surface of a silica gel. Chelation groups can be bond with silica gel to extract metal ions from wastewater [43-44].

2.5.2 Chelating material advantages

1. High specific surface area (750 to 800 m^2/g).
2. 2-Act as drying agent
3. Absorbing moisture.
4. Material silica gel removes moisture by adsorption onto the surface
5. Absorption into the bulk of the gel
6. High mechanical and thermal stability.
7. Easily modified with functionalized silanol.

8. Resistant to removal from the surface by organic solvents.
9. Modified silica can have operated without loss of the expensive organic molecules.

2.5.3 Preparation of a solid support matrix immobilized ligand system

The reaction of activated silica gel with 3-aminopropyltrimethoxysilane in toluene for amino groups bind to the silica surface (3-aminopropylsilica (Si-NH₂)). Then these NH₂-groups reacted with 1,5-dimethyl-1*H*-pyrazole-3-carbaldehyde under mild conditions (reflux, atmospheric pressure and 8 h) to form the modified chelating sorbent SiNP. Anhydrous ethanol used as solvent.

2.6. Methodology of preparing a solid support matrix surface modified with 1,5-dimethyl-1-*H*-pyrazole-3-carbaldehyde

The synthetic procedure summarized in the following figure 1 [45].

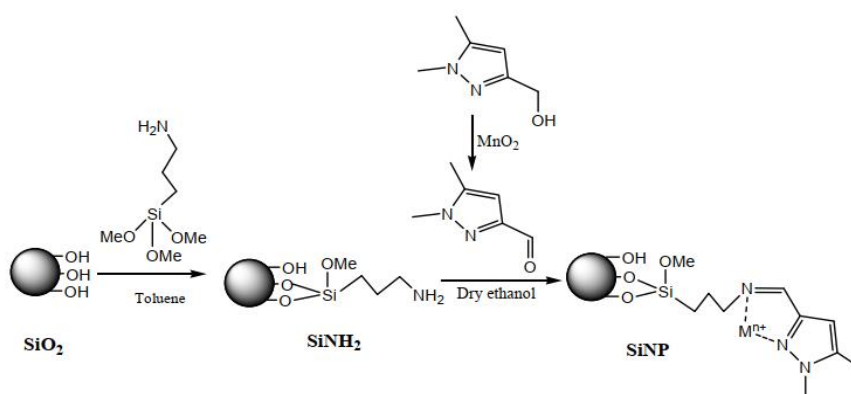


Figure 2: summarize OF synthetic procedure

The synthesis done by Professor Smaail Radi from university of Mohammed premier university in Oujda, Morocco.

Higher amount of the inorganic components such as copper ions will form available chelation sorbent of SiNP. Copper ions were chelated on the SiNP as a new chelating matrix, because of two amine groups are present on the TMP and it could chelation occur between the amines and the copper ions of the adsorbents. This new chelating material with copper ions will use as an adsorbent for removal **TMP** from wastewater.

2.7 Computational details

2.7.1 DFT part

All density functional theory (DFT) calculations were performed using Gaussian 09 package [46]. The geometry of **TMP** was optimized using the B3LYP exchange correlation functional level without constrains [47-49]. The 6-31+g(d,p) basis set has been utilized for this work [50]. For the solvation effect, the self-consistent reaction field (SCRF) method was employed using the polarizable continuum model (PCM) solvation method. Frequency calculations were also employed at the same level to depict the stationary points and confirm that the ground states have no imaginary frequency[51-53]. By using the highest occupied and the lowest unoccupied molecular orbitals energies (E_{HOMO} and E_{LUMO}) of the optimized structure, some of the energy gap ($\Delta E = E_{LUMO} - E_{HOMO}$), electronic chemical potential ($\mu = \frac{1}{2}(E_{LUMO} + E_{HOMO})$), global hardness ($\eta = \frac{1}{2}(E_{LUMO} - E_{HOMO})$), hyper-hardness ($\gamma = E_{LUMO} - 2E_{HOMO} + E_{HOMO-1}$), softness ($S =$

$1/\eta$), electrophilicity ($\omega = \mu^2/2\eta$) and maximum charge transfer ($\Delta N = -\mu/\eta$) are calculated for **TMP** molecule[54-55].

The local reactivity descriptors (LRD) for nucleophilic attacks ($f_k^+ = q_k(N+1) - q_k(N)$) and for electrophilic attacks ($f_k^- = q_k(N) - q_k(N-1)$) of **TMP** were calculated by means of the Fukui functions (FF) [56-57]. The $q_k(N)$, $q_k(N+1)$ and $q_k(N-1)$ are charges values of atom (k) for neutral, cation and anion species, respectively. These indices numerically signify the most reactive centers that are responsible for the interactions with **SiNP** surface. Additionally, the local softness ($\sigma_k^\alpha = sf_k^\alpha$) and local electrophilicity ($\omega_k^\alpha = \omega f_k^\alpha$) were also calculated [58]. The letter $\alpha = (+)$ and/or $(-)$ describes the nucleophilic and electrophilic attacks, respectively. More precisely and to get a clearer identification for the electrophilic and the nucleophilic attack at specific atomic sites [59-60], the dual descriptors (DDs) (Fukui descriptor or the second order Fukui functions ($f_k^2 = f_k^+ - f_k^-$), the dual softness ($\Delta\sigma_k = \sigma_k^+ - \sigma_k^-$) and the dual philicity $\Delta\omega_k = \omega_k^+ - \omega_k^-$) were also calculated. These DDs give simple way to chemical reactivity in a local sense and allow us to attain instantaneously the preferably sites for nucleophilic attacks and the preferably sites for electrophilic attacks ($f_k^2, \Delta\sigma_k$ and $\Delta\omega_k < 0$) [59-61].

Chapter Three
Experimental Part

Chapter Three

Experimental Part

3.1 Chemicals and Materials

The pharmaceuticals and organic chemicals were of high purity, (purity > 99.5 % and they were purchased from Aldrich, Saint-Louis, MO, USA), and all of them used without purifications. The silica gel and the silylating agent 3-aminopropyltrimethoxysilane were purchased from Janssen Chimica, Geel, Belgium and used without purification.

3.2 SiNP Synthesis:

For Synthesis of 1.5-Dimethyl-1H-pyrazole-3-carbaldehyde, 1.2 g, (9.52 mmol) of 1.5-Dimethyl-1H-pyrazol-3-yl) methanol was dissolved in 100 ml of 1,4-dioxane. Then added 21.88g of activated manganese dioxide to the solution with stirring under reflux for 5 h. TLC (alumina, CH₂Cl₂ as eluent) used for monitoring the reaction. The filtrate MnO₂ was washed with heated 1,4-dioxane and the solvent was removed using a rotary evaporator to produce a product as a liquid (0.7 g, yield 59.23%).

Both silylating agent and silanol groups were reacted using the silica surface and refluxed. The silica gel was washed with dried toluene (150 mL) with continuous stirring under nitrogen atmosphere for about 2 h. The aminopropyltrimethoxysilane (10 mL) was then added dropwise to the reaction followed by refluxing for 24 h. After that filtration and washing with toluene and ethanol mixture. The silylating reagent was removed

using 1:1 mixture of ethanol and dichloromethane. The product will be 3-Aminopropylsilica (SiNH₂).

A mixture (SiNH₂, 5 g) and 1.5-dimethyl-1*H*pyrazole-3-carbaldehyde (3 g) with ethanol (60 mL) were stirred and refluxed for 8 h . After filtration and extraction with acetonitrile followed by methanol the final solid product is called SiNP. The synthesis done by Professor Smaail Radi from university of Mohammed premier university in Oujda, Morocco.

3.3 Preparation of Trimethoprim solutions

Exactly 0.25 g of **TMP** was taken in a 250 mL volumetric flask and diluted up to the mark (we obtained 1000 mg/L **TMP** solution). By dilution prepared 5, 10, 15, 20, 30 mg/L **TMP** solutions.

3.4 Calibration Curve

The concentration of several **TMP** solutions analyzed by UV-Vis at 264 nm.

Calibration curve between absorbance and concentration obtained in the range 5-30 mg/L **TMP** solution, as shown in Figure 2: calibration curve between absorbance vs concentration for **TMP** concentrations in the range 0-30 mg/L

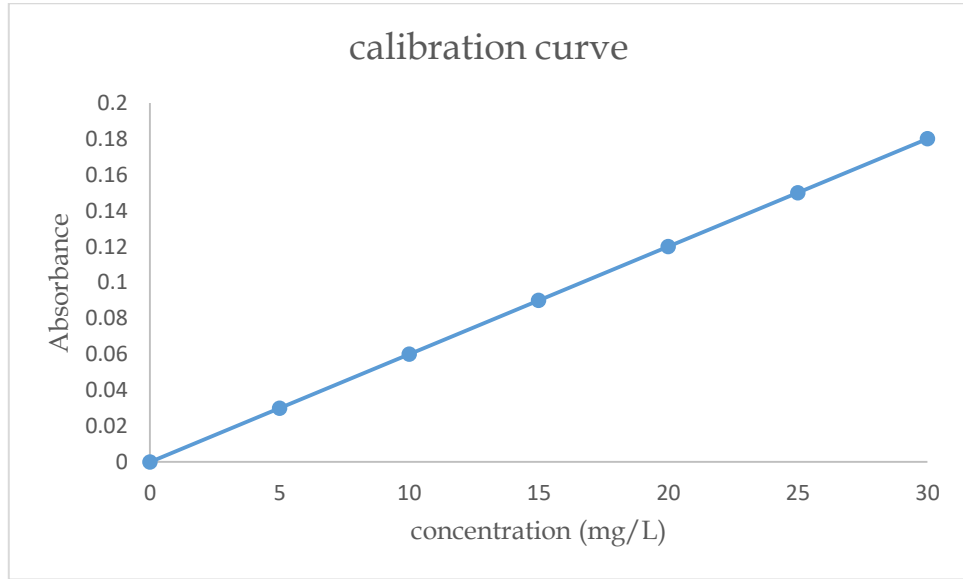


Figure 3: calibration curve between absorbance vs concentration for TMP concentrations in the range 0-30 mg/L

3.5 Adsorption Experiments

For pH adjustment, Hydrochloric acid (0.1M) and sodium hydroxide (0.1M) used. The efficiency of the absorption estimated by batch experimental studies. The adsorption behavior of the surface with **TMP** solutions studied. The effect of contact time, temperature, pH, dose of adsorbent, and the concentration of **TMP** solutions on the adsorption process studied. Adsorbent removed by filtration.

The adsorption capacity of the **TMP** for the **TMP** calculated using the following equation 3-1 [62]:

$$q_t = \frac{(C_0 - C_t)}{m} v \quad (3-1)$$

C_0 is the initial **TMP** concentration (ppm) and C_t (ppm) is the residual **TMP** concentration at time t . C_e is the final **TMP** concentration in the sample solution after filtration.

The removal capacity (q_e , mg/ g) quantified by equation 3-2:

$$q_e = \left[\frac{(C_o - C_e)}{m} \right] \times v \quad (3-2)$$

Where q_e : amount of adsorbed TMP at equilibrium, V (L) is the volume solution of TMP, m (mg): mass of the used modified (SiNP).

The correlation coefficient (R^2) used to determine the best fitting isotherm, q_m is the constant, q_e is the equilibrium capacity q_e^- is the average of q_e . The correlation coefficient (R^2) equation shown below in equation

(3-3):

$$r^2 = \frac{\sum(q_m - q_e^-)^2}{\sum(q_m - q_e^-)^2 + \sum(q_m - q_e)^2} \quad (3-3)$$

3.5.1 Experiment (1): Optimize the contact time

A 50 mL of TMP solution (10 mg/L) taken and put in 100 mL beaker with 0.03 g of adsorbent. At different time intervals, part of the supernatant taken using the pipette and residual concentration of TMP measured by UV-Vis at normal pH.

For each experimental, three samples taken and the average reported.

3.5.2 Experiment (2): pH value effect

The effect of pH on adsorption process measured in range 2-12. The pH adjusted using 0.1M NaOH and 0.1M HCl. A 50 mL of (10 mg/L) TMP added to 0.03 g adsorbent. The sample then put in

shaking water bath for 100 min at 25°C. At the end, adsorbent removed by filtration then filtrate measured by UV-V for the residual concentration of **TMP**.

3.5.3 Experiment (3): Temperature effect

The effect of temperature on adsorption process studied in the range 25-45°C. A 50 mL of (10 mg/L) **TMP** solutions added to 0.03 g adsorbent samples at pH 8. Each sample put in shaking water bath at required temperature for 100 min.

Finally, adsorbent removed by filtration then filtrate analyzed by UV-Vis.

3.5.4 Experiment (4) Trimethoprim initial concentration effect

TMP initial concentration effect on adsorption process investigated. A 50 mL of several concentration of trimethoprim solution (5-30 mg/L) added to 0.03 g of adsorbent, under optimized temperature (25°C) and pH 8 for 100 min. The absorbance of filtrate measured by UV-Vis.

3.5.5 Experiment (5) - Adsorbent dose effect

Adsorbent dose effect on the adsorption of **TMP** investigated.

In order to detect optimum dose. A 50 mL of 10 mg/L trimethoprim solutions added to 100 mL beakers containing 0.01, 0.03, 0.07, 0.1 and 0.15 g of adsorbent at pH 8. The samples were put in shaking

water bath at 25°C for 100 min. Absorbance of the filtrate was measured by UV-Vis.

3.6 Kinetics and Thermodynamics of Adsorption

Pseudo-first order and pseudo-second order kinetic models investigated from studying contact time effect on **TMP** adsorption at Si-NP. The Parameters for adsorption of **TMP** at Si-NP were determined. The value of both experimental and calculated q_e compared.

The adsorption behavior of adsorbent with **TMP** studied. We are trying to reach optimum adsorption conditions by studying the effect of: pH, contact time, adsorbent dose, temperature and initial concentration of **TMP**. Concentration of **TMP** measured before and after adsorption by using UV-Vis. Langmuir, Freundlich adsorption isotherm equations were studied. The values of corresponding parameters were determined. Thermodynamic parameter like (ΔS°), (ΔH°), and (ΔG°) were evaluated employing Van't Hoff's equation. At different temperatures ranging (308–320K), the values of K_C and percentage removal for trimethoprim were calculated.

Chapter Four

Result and Discussion

Chapter Four

Result and Discussion

4.1 Characterization:

4.1.1 FT-IR Characterization

A Perkin–Elmer FT-IR spectrophotometer (Spectrum BX-II) was used to record FT-IR spectra on KBr disks. with a range of 4000–400 cm^{-1} .

To study the synthesis of new materials that has been synthesized for TMP removal (SiNP-Cu) it is necessary to study the functional groups. Si-O-Si stretching vibrations peak appear at 1,100 cm^{-1} . The presence of vibration peaks at 3446 and 1620 cm^{-1} confirmed presence of adsorption water. The presence of SiNP may be determined by analyzing the appeared bond about 1,4900 cm^{-1} , which reflects the bonds of C=N and C=N vibrations. This validates the molecule's functioning via the silica surface. FT-IR Spectra of SiG, SiNH₂ and SiNP shown in figure 4.1.

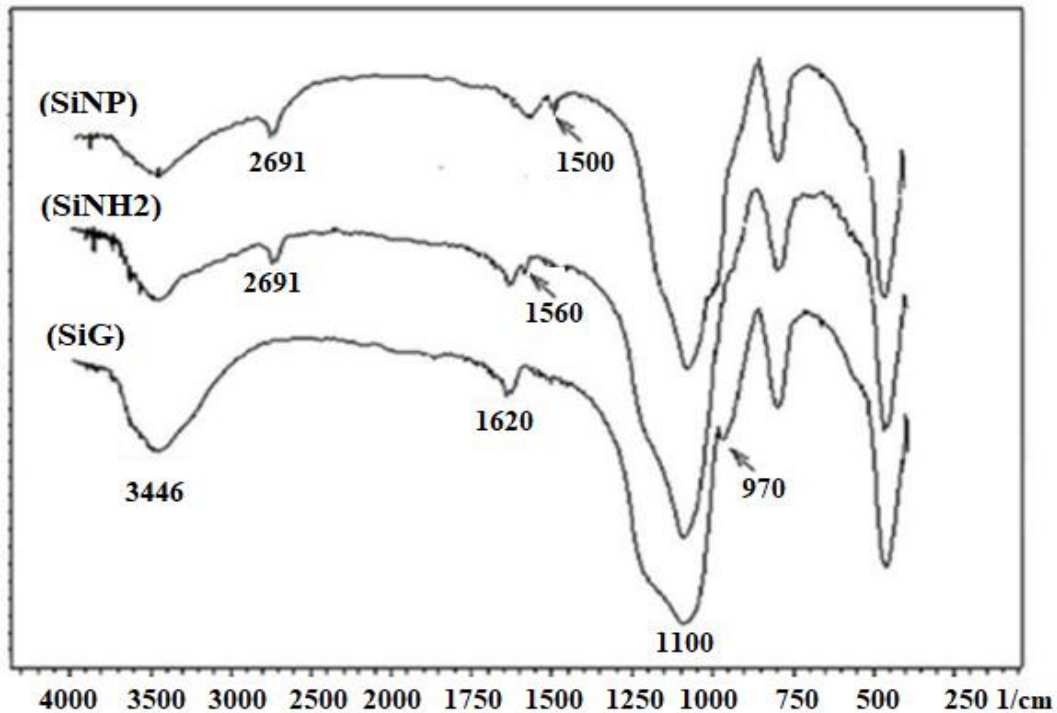


Figure 4: FT-IR Spectra of SiG, SiNH₂ and SiNP

4.1.2 Scanning Electron Micrographs

Scanning electron micrographs (SEM) of SiNP and SiNP-Cu were obtained using a scanning electron microscope (Jeol JSM 60) and an accelerating voltage of 20 kV.

The SEM is shown in Figure 4.2 were obtained at 800 X magnification. From the SEM we can see the rough surface for the new synthesized functionalized structures were present on the surface equally. This demonstrated the inalienability of the silica gel species after curing to demonstrate the presence of functional group distribution on the entire surface. In addition, we can see in portion (a) that the copper ions were spread equally. SEM images of SiNP (A), SiNP-Cu (B) shown in figure 4.

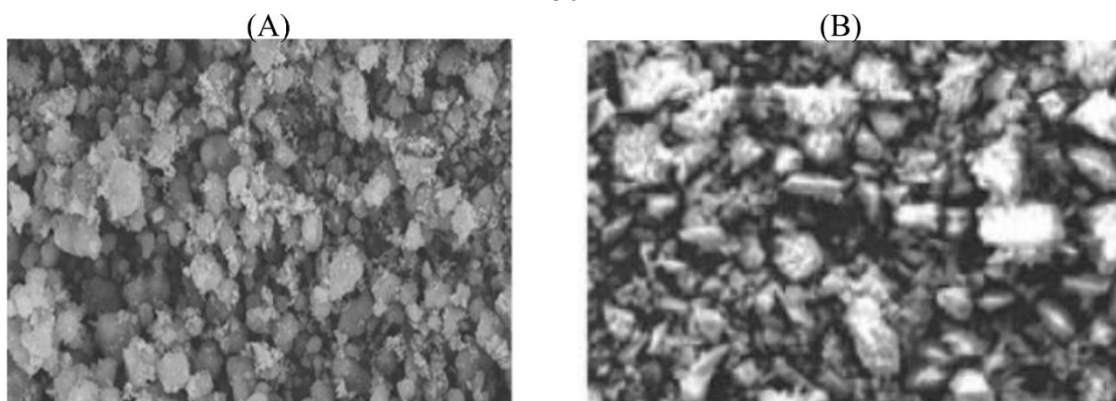


Figure 5 : . SEM images of SiNP (A), SiNP-Cu (B)

4.1.3 TGA Analysis and Thermal Stability

For mass loss and stability studies, A dry sample was heated in a nitrogen gas at a rate of 10 °C/min (flow rate: 50 mL/min).

This study will help us to have an idea about the surface stability and at the same time to be sure there is mobility on the surface and how much. According to the profiles in a and c, the degradation process occurred between 120 and 800 °C, demonstrating that both SiNP and SiNP-Cu produced materials had high thermal stability. TGA analysis of free silica (a), of SiNP (b), SiNP-Cu (c) shown in figure 5.

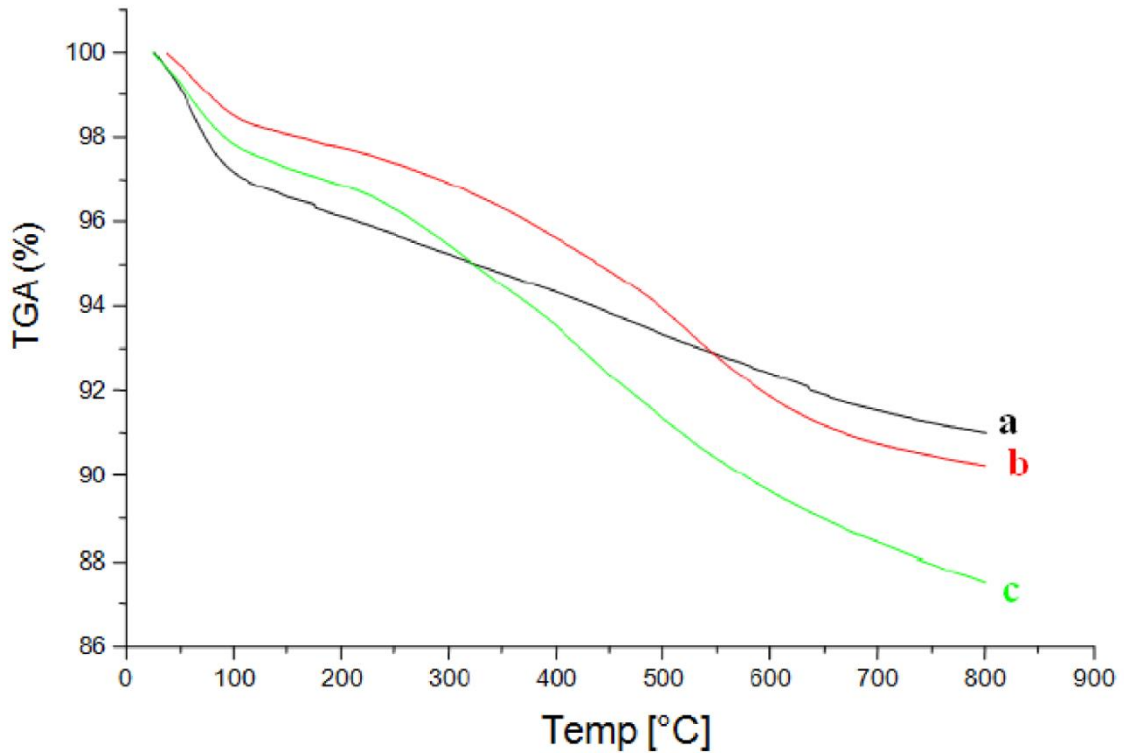


Figure 6: TGA analysis of free silica (a), of SiNP (b), SiNP-Cu (c)

4.2 Investigation of adsorption parameters

4.2.1 Contact time effect on TMP adsorption

Contact time effect on **TMP** adsorption on SiNP bond with copper ions, for different temperatures to determine the maximum time of adsorption, as shown in Figure 6. During the first 25 min, rapid adsorption of **TMP** detected, which resonated to copper ions in the matrix, then decreasing removal rate with time.

These results were taken at equilibrium when **TMP** concentration was reached. From the results, the equilibrium time was set to 100 min for the rest of the SiNP bath experiments to make sure that equilibrium is reach.

During the time, increase the adsorption of trimethoprim with time was detected on three temperatures were studied, which resonated to

coppers chelate in the matrix. At the first, all the reacting sites are vacant, so, the rate of adsorption capacity is high and the adsorbents have available high surface area for adsorption of **TMP**, and the absence of different internal diffusion resistance for the solution. The slow removal rate at the end may encourage of formation of a monolayer of **TMP** outside the surface of **SiNP**, and intra particle diffusion onto the inner surface. The adsorption becomes constant because of adsorptive sites were filled. The adsorption process for **TMP** at various temperatures gradually reached equilibrium by 100 min. From the figure 6 we can see the same equilibrium times for the temperatures studied, and not significant increase in the percentage adsorption with increase temperature.

Effect of contact time of TMP adsorption on SiNP is show in the Figure 6 below:

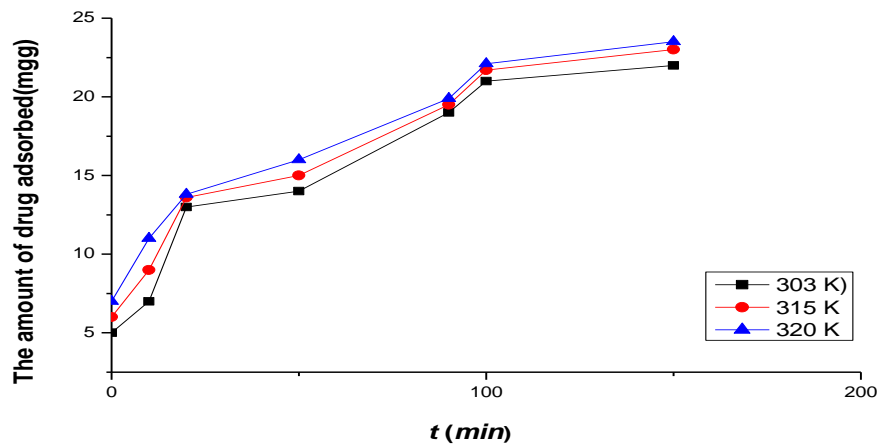
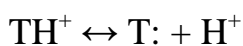


Figure 7: Effect of contact time of TMP adsorption on SiNP

4.2.2 pH effect on TMP adsorption

pH is important factor, which is the rate of adsorption process affected. The pH effect on removing TMP by modified SiNP at equilibrium nearly between 2 and 12 is represented in Figure7. The adsorption process of TMP were affected with an increase of pH. The TMP adsorption using the synthesized SiNP increases nearly between a pH between 2 and 12 leads to a maximum value around 8 and does not change considerably for higher pH values. Upon increasing the pH of the solution from 2 to 8 the removal capacity was increased from 35% to 88%. This is due to the electrostatic forces of attraction between adsorbent and adsorbate. The TMP is considered a weak base with a pka of 7.4. At low pH conditions ($\text{pH} < \text{PKa}$) TMP (T:) is in the protonated form :



The adsorbent surface that has positive charge (from copper ions), can act as a Lewis acid, (accepting electrons from the amine groups of TMP) does not prefer the protonated form of the drug. TMP at acidic pH values carrying positive charge , that may explain the poor adsorption of TMP on the surface of SiNP. The percentage of adsorption is increased with an increase in pH , because of deprotonated form of the drug at higher pH values($\text{pH} > \text{pka}$) , the net positive charge decreased while increasing pH value that leads in the decrease of repulsion between the adsorbent surface and TMP and this will improve the adsorption capacity. The adsorption mechanism based on chelation between the amine group of the TMP with the metal . Chelation may be responsible for the higher pH of the suspension during the isotherm measurements, so the adsorption studies were carried out at high pH for SiNP bond with copper sorbents. From the figure the optimal pH value for the adsorption was 8.

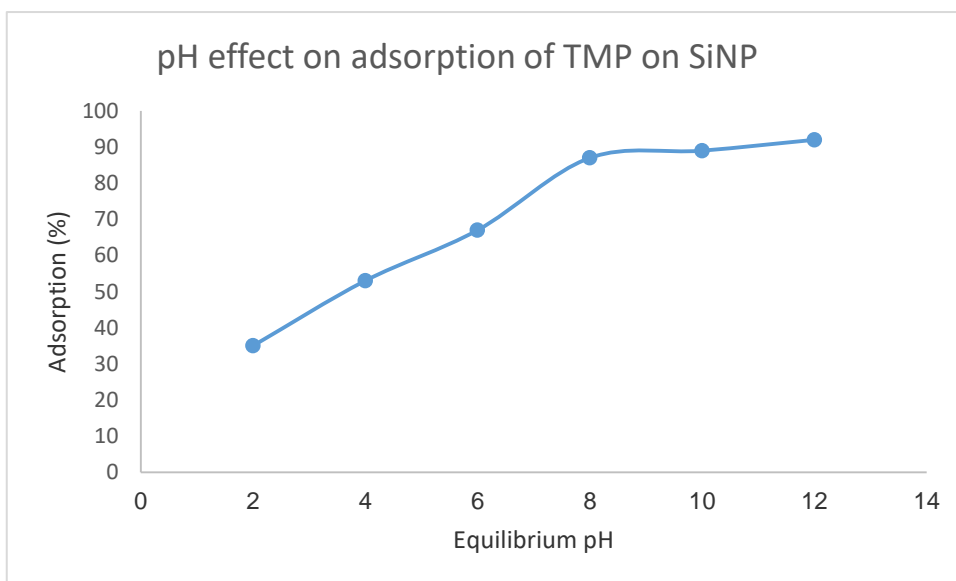


Figure 8: pH effect on adsorption of TMP on SiNP

4.2.3 Temperature effect on TMP adsorption

Temperature plays a critical role in any kind of adsorption processes. To measure adsorption isotherms and thermodynamic parameters, usually same procedures were used at various temperatures of 308, 315 and 320 K. The change in the adsorbed amount of TMP with equilibrium concentrations was shown in figure 8.

The variables C_s was the solid phase concentration (m mol g^{-1}) and C_e was representing the final concentration (m mol L^{-1}) in the supernatant at equilibrium for each initial concentration. From the figure 4.6, both the adsorption amount and rate of TMP using synthesized SiNP enhanced following an increase in temperature from 308 to 320 K, explaining that temperature had a positive effect on adsorption. Beside the removal efficiencies and capacities of the target antibiotics at different temperatures (308, 315, 320 K) increased significantly at the first few minute and this caused by large amount of vacant active sites. And also the surface area on the SiNP beside the total pore volume of the adsorbent during increasing the temperature. These results lead to an endothermic nature.

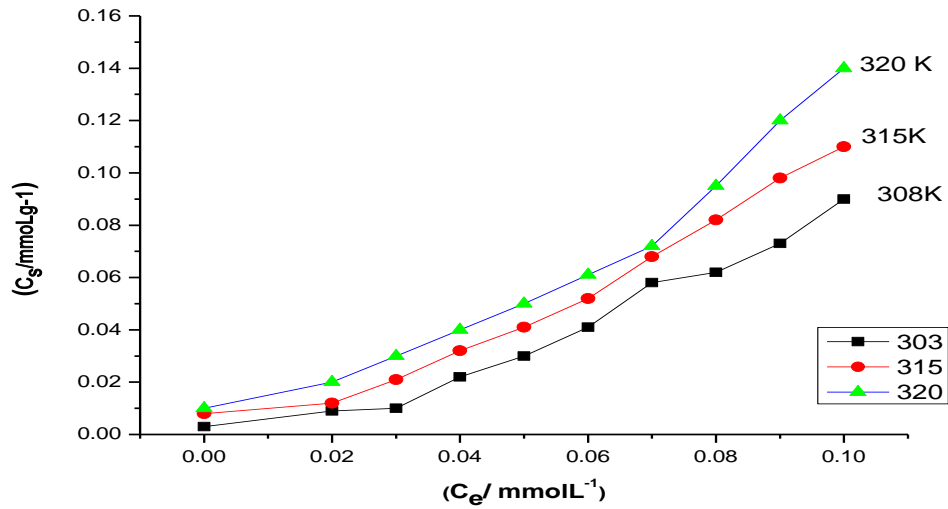


Figure 9: Temperature effect on adsorption process

4.2.4 TMP concentrations effects

TMP concentration was calculated from the absorption of the sample solution at 264 nm based on Beer-Lambert law. Effect of initial concentration of TMP on adsorption process was investigated for concentration from 10 to 50 ppm with fixing previous conditions like contact time, volume of solution, temperature and pH. Regarding to maximum removal of TMP at 10 ppm. Concentration of analytes 10 ppm, chosen as the optimal concentration.

4.2.5 Adsorbent dose effect

Effect of adsorbents dose on adsorption processes was studied with fixing all Previous conditions like contact time, volume of solution, temperature, pH, initial concentration of TMP. Adsorbent dose effect is important factor because of the amount of adsorbent determines the capacity of an adsorbent. The removal and adsorption

percentage of the synthesized SiNP usually increased with increasing adsorbent dosages from 0.1 to 0.3g due to the increase in the number of reaction sites available to TMP. This leads to an increased percentage of TMP removal from the solution. The adsorption dose effect shows in figure 9.

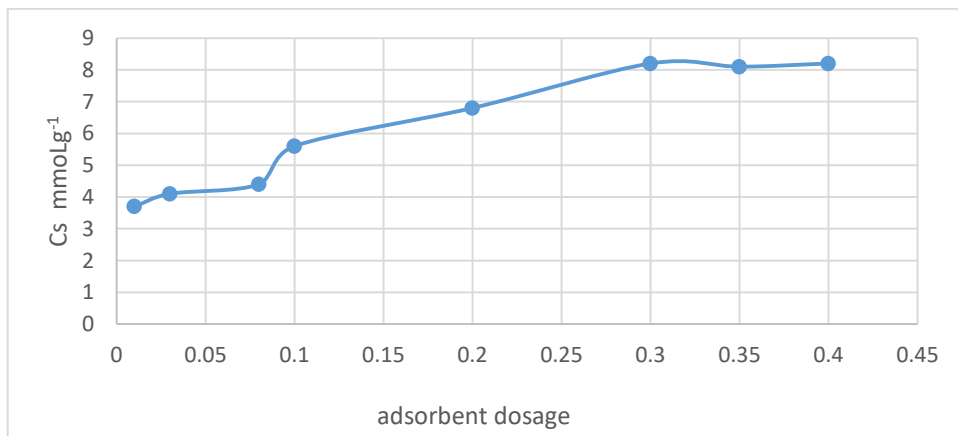


Figure 10: Effect of adsorbent dose on the adsorption process

4.3 Adsorption isotherm of trimethoprim

The most common available isotherm equations to evaluate experimental sorption process parameters are the Langmuir or Freundlich models.

4.3.1 Langmuir Adsorption Isotherm

Langmuir isotherm model used to describe the chemisorptions and the affinity for adsorption of a mono- layer molecular. In Langmuir isotherm model, there are no interaction between the adsorbed molecules.

The famous linear Langmuir equation can have expressed in equation below.

$$\frac{C_e}{C_s} = \frac{1}{C_m \alpha_L} + \frac{C_e}{C_m} \quad (4-4)$$

Where: C_m is the amount of **TMP** necessary for the formation of the monolayer (adsorption capacity). C_s is the solid phase concentration (m mol/g). C_e is adsorbate concentration at equilibrium (m mol/L). α_L is represent the Langmuir constant (L/mg) related to the intensity and energy of the adsorption. The specific sorption (C_e/C_s) plotted against the equilibrium concentration (C_e), for each specific temperature studied. From the plot, the values of the constants C_m and α_L were found.

From Langmuir plot, the values of C_m , α_L , and R^2 were determined as shown in figure 10 . Langmuir plot for TMP adsorption on modified (SiNP).

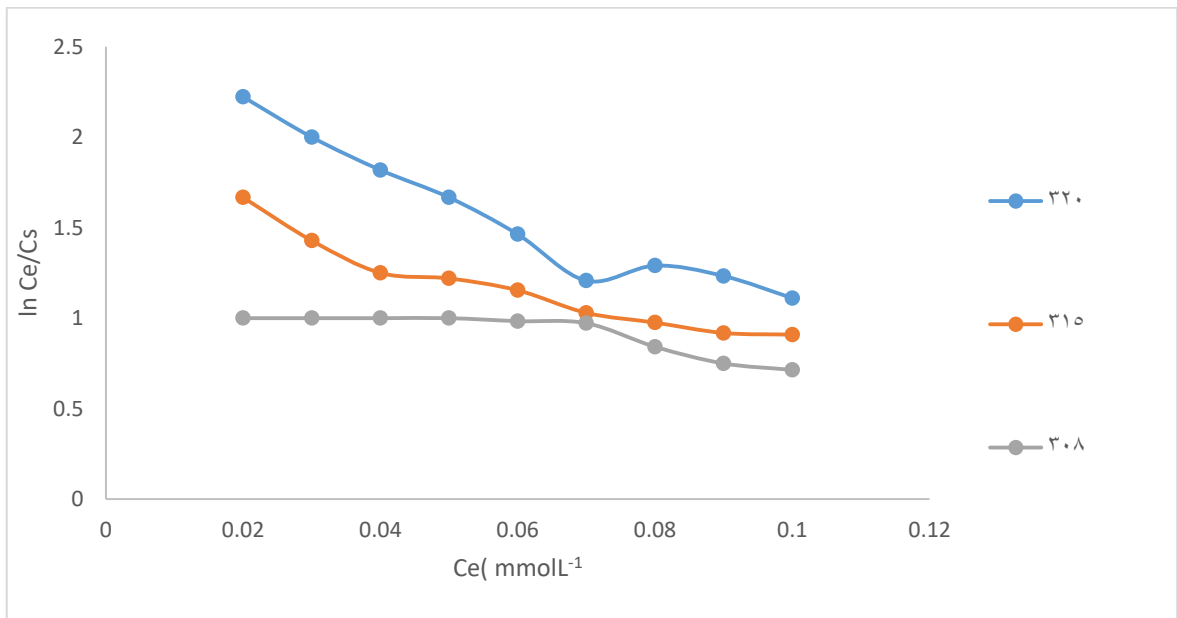


Figure 2: Langmuir plot for TMP adsorption on modified (SiNP)

The values of these parameters shown in table 4. All C_m values were negative for modified SiNP.

Table 4: Langmuir isotherm and correlation coefficient parameters of adsorption of trimethoprim on modified (Si NP)

Langmuir isotherm parameters	At T=308K	AT T=315 K	AT T=320 K
slope	-18.769	-8.833	-3.7274
intercept	2.7941	1.7023	1.1417
R^2	0.7044	0.9151	0.7604
C_m (mmol/g)	-0.05328	-0.11321	-0.26828
α^L (gL^{-1})	-6.71737	-5.18886	-3.2647
R_L	4.28	2.16	2.32

4.3.2 Freundlich Adsorption Isotherm

The Freundlich isotherm model indicate exponential distribution of the active site and energies surface heterogeneity of the adsorption intensity. Such model take place when the adsorbate concentration increase with increasing adsorbate concentration on the adsorbent surface. The famous expression for the Freundlich isotherm model given as in equation:

$$\ln C_S = \ln K_f + n_f \ln C_e \quad (4-3)$$

Where K_f is represents the adsorption capacity and n_f is a characteristic constant representing sorption intensity, C_s , C_e and K_F represent sorbent amount (m mol/g), residual concentration of sorbet in solution at equilibrium (m mol/L) and sorption capacity of sorbent (m mol /g) respectively. Freundlich plot for TMP adsorption on (Si-NP) showed in figure 11 bellow:

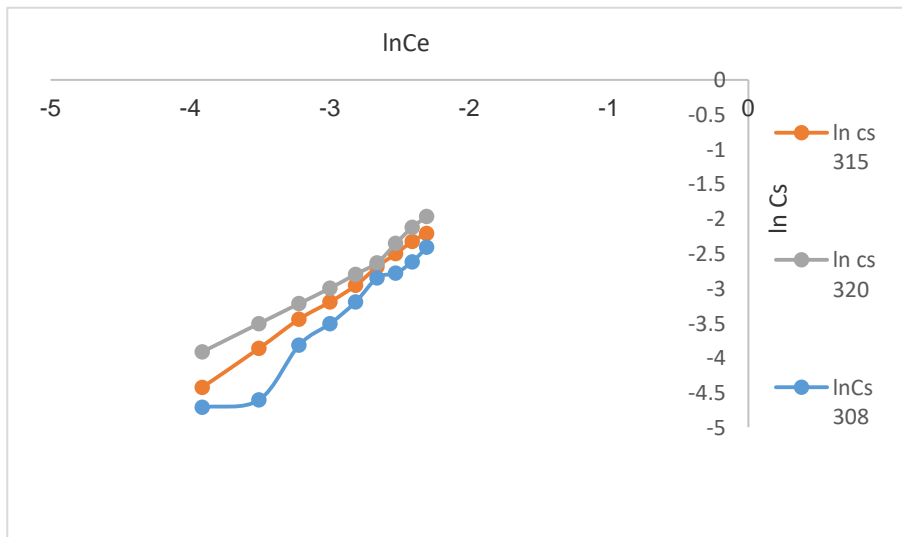


Figure 12: Freundlich plot for TMP adsorption on (Si-NP)

The values of Freundlich constants n_f , K_F and regression constant (R^2) shown in Table 5.

Table 5: Freundlich isotherm parameters and correlation coefficient for adsorption of trimethoprim on (Si-NP)

Freundlich Adsorption Isotherm			
Temp.(K)	308	315	320
Slope	1.3817	1.3817	1.1902
Intercept	0.9778	0.9778	0.6502
R^2	0.9989	0.9989	0.9805
n_f	1.3817	1.3817	1.1902
K_F	2.658	2.65	1.9159

As shown in table 5, K_F values decreased by during increasing temperature and this suggest that when we have a lower temperature (308K) this will cause a higher affinity of the synthesized SiNP for the TMP. From the values of R^2 , Freundlich model yielded a much better fit than the Langmuir model. This explained that the boundary layer thickness probably increased, and may be the adsorption has several layers on the top of sorbents surface. The value of n is close to unity, which means a good adsorption. The calculated n value for the adsorption of TMP was between 1.19 - 1.38 showing a good efficiency for TMP adsorption by SiNP adsorbent.

These results indicate that SiNP had strong adsorption capacity for TMP in the solution.

Table 6: correlation coefficient and parameters of Langmuir, Freundlich for adsorption of TMP on (Si-NP) at 308, 315, 320 K.

Langmuir isotherm parameters	Temp.(K)	C_m (m mol/g)	α_L (L/mg)	R^2
	308	-0.05328	-6.71737	0.7044
	315	-0.11321	-5.18886	0.9151
	320	-0.26828	-3.2647	0.7604
Freundlich isotherm parameters	Temp.(K)	n_f	K_F	R^2
	308	1.3817	2.658	0.9989
	315	1.3817	2.65	0.9989
	320	1.1902	1.9159	0.9805

The adsorption data suited with Langmuir and Freundlich, but Freundlich adsorption model found to be with highest R^2 and from here the best suit. The Freundlich model fit more with the experimental data of adsorption indicates physical adsorption in addition to heterogeneon mode distribution of adsorbate active sites at the adsorbent surface.

4.4. Adsorption thermodynamics

Thermodynamic parameters using to study adsorption of TMP by (Si-NP) were calculated using equations:

$$Kc = \frac{C_s}{C_e} \quad (4-4)$$

$$\Delta G^\circ = -RT \ln Kc \quad (4-5)$$

$$\ln Kc = \left(\frac{\Delta S^\circ}{R} \right) - \left(\frac{\Delta H^\circ}{RT} \right) \quad (4-6)$$

Where K_C : the equilibrium constant, ΔG° : the Gibbs free energy in J/mol, ΔS° : the entropy change in J/mol. K.

R: the universal gas constant in J/mol. K. T is the absolute temperature in K and ΔH° is the enthalpy change in kJ/mol.

From the plot of $\ln K_C$ vs. $1/T$ in figure.4.10, the intercept and slope found and the values belong to entropy change (ΔS°) and enthalpy change (ΔH°) were calculated. The values of Gibbs free energy (ΔG°) calculated at different temperatures.

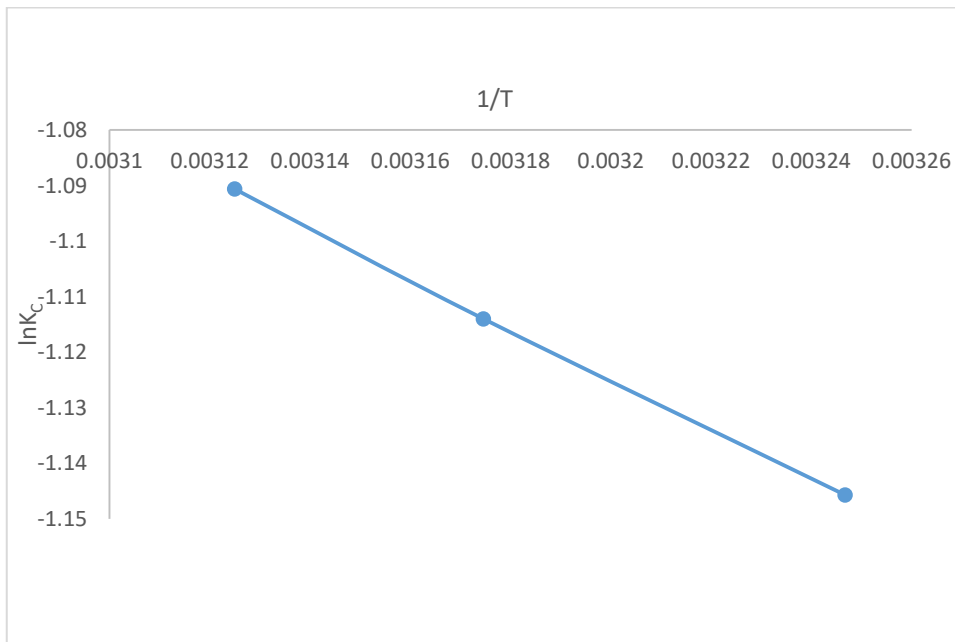


Figure 13: Adsorption thermodynamics of TMP onto SiNP

The results exhibit that ΔS° was 2.771 J/ mol K, ΔH° was 3.785 kJ /mol. ΔG° at different temperatures calculated from the following equation:

$$\Delta G^\circ = \Delta H^\circ - T\Delta S^\circ \quad (4-7)$$

The thermodynamic parameters on TMP adsorption shown in table 7:

Table 7: The thermodynamic parameters on TMP adsorption

ΔS° (J/mol .K)	ΔH° (J/mol)	ΔG° (J/mol)		
		308K	315K	320K
2.7718	3785.45	2933.818	2975.905	2901.637

The positive value of ΔG° at several various temperatures showing the nature of adsorption is not spontaneous.

From Table 7, the value of ΔH° is positive and also, the vant Hoff plots of the interaction of the TMP with the surface of the adsorbents usually require enough energy and this is the nature of endothermic which cause an increase in adsorption during increasing temperature. Several parameters that lead to low adsorption enthalpy such as physical interactions which caused from electrostatic and nonpolar physical interactions, water bridging, hydrogen type bonding is another parameter, and finally ion-exchange reactions between the TMP molecules and the adsorbent surfaces.

The value and sign of the entropy (ΔS°) gives information if the adsorption process is an associative or in the other hand dissociative process. From the Table, the standard entropy change for TMP sorption process is positive which explain the degrees of freedom for the adsorbed species are usually increasing with dissociative process.

4.5 Adsorption kinetics of TMP

The kinetics study of TMP onto SiNP has analyzed at concentration of 25 ppm with respect to different adsorption temperature from 308 to 320 K. The adsorption kinetics investigated with Lagergren's pseudo first-order and second order model.

The pseudo-first order kinetic model of Lagergren's expressed below:

$$\frac{1}{q_t} = \left(\frac{k_1}{q_1}\right) \left(\frac{1}{t}\right) + \frac{1}{q_1} \quad (4-8)$$

Where q_t : the amount of solute adsorbed at various time t , in (mg/g), q_1 : the maximum adsorption capacity (mg/g) and k_1 : first order rate constant (min^{-1}).

Kinetic parameter k_1 and q_1 calculated from the slope and intercept of the pseudo first –order straight line in figure 13. These parameters and correlation coefficients (R_1^2) were determined in Table 8. R_1^2 were between 0.5422 and 0.9044 at 308, 315, and 320 K, respectively. Pseudo first order model is suitable to TMP adsorption on SiNP if plot was having good correlation coefficient close to one. From the table, the adsorption process is not pseudo first order process. Calculated and experimental q_1 value were represented in table 8 shows that the calculated q_e values are not compatible with the experimental q_e value. This indicate that the pseudo first –order kinetics not good fit for this process.

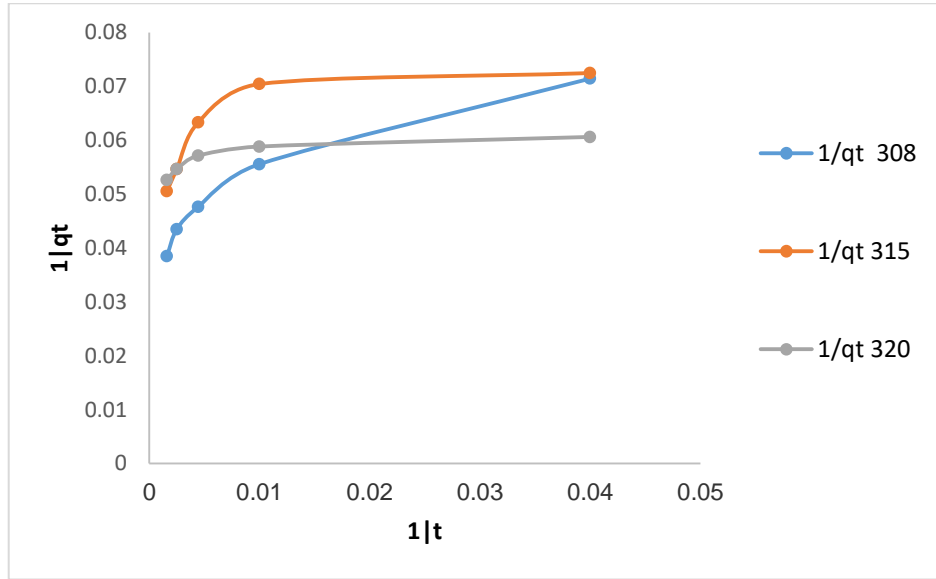


Figure 3: A pseudo-first order kinetic model

The pseudo -second-order kinetic model known equation related to equilibrium adsorption as in equation (4-9).

$$\frac{t}{q_t} = \frac{1}{k_2 q_2^2} + \frac{t}{q_2} \quad (4-9)$$

K_2 is the rate constant at equilibrium ($\text{g mg}^{-1}\text{min}^{-1}$). q_2 is the maximum adsorption capacity (mgg^{-1}). From the linear plots of (t/q_t) versus t . K_2 and q_2 at various temperatures calculated.

From the plots and fitting equations, the calculated data showed that the adsorption process of TMP onto SiNP followed the pseudo-second – order kinetic model. The calculated adsorption capacity was almost near the experimental values, so the adsorption may be in the active parts of the sorbents surface.

The experimental data fitted better by the second-order kinetic model as seen from Table 8. Calculated and experimental q_2 values are compatible.

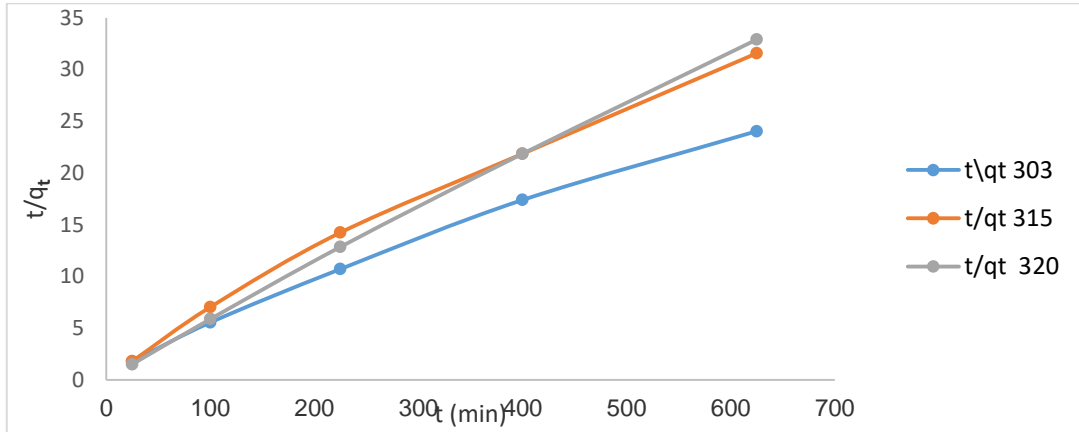


Figure 15: the second order kinetic model

The maximum adsorption capacities measured from TMP adsorption onto SiNP lower at high temperature. This explain that the adsorption of TMP is a physical process adsorption.

Table 8: The kinetic parameter for TMP adsorption on SiNP

Pseudo first order	Temp.(K)	308	315	320
	K_1	17.8797	7.660	2.8597
	q_e	23.5849	17.51313	18.2149
	Q_e (calculated)	9.32	11.23	13.62
	R^2	0.9044	0.5422	0.6311
Pseudo second order	Temp.(K)	308	315	320
	K_2 ($gmg^{-1}min^{-1}$)	0.00078	0.0012	0.00415
	q_e (mgg^{-1})	27.1002	20.5338	19.1570
	q_e (calculated)	42.86	22.23	47.85
	R^2	0.9919	0.9919	0.999

Other model applied in order to quantify the changes in adsorption with time. Intra particle diffusion model of Weber and Morris [63] shown in equation (4-10):

$$qt = kt^{1/2} + C \quad (4-10)$$

Q_t : the amount of drug adsorbed (mol/g) at time t , C is the intercept, that give an idea about the boundary layer thickness. k_i is the intra particle diffusion rate constant ($\text{mg s}^{-1} \text{g}^{-1}$). From the plot of q_t versus $t^{1/2}$, k_i value obtained. Intra particle diffusion model given in Equation (4-10) shown in figure 15.

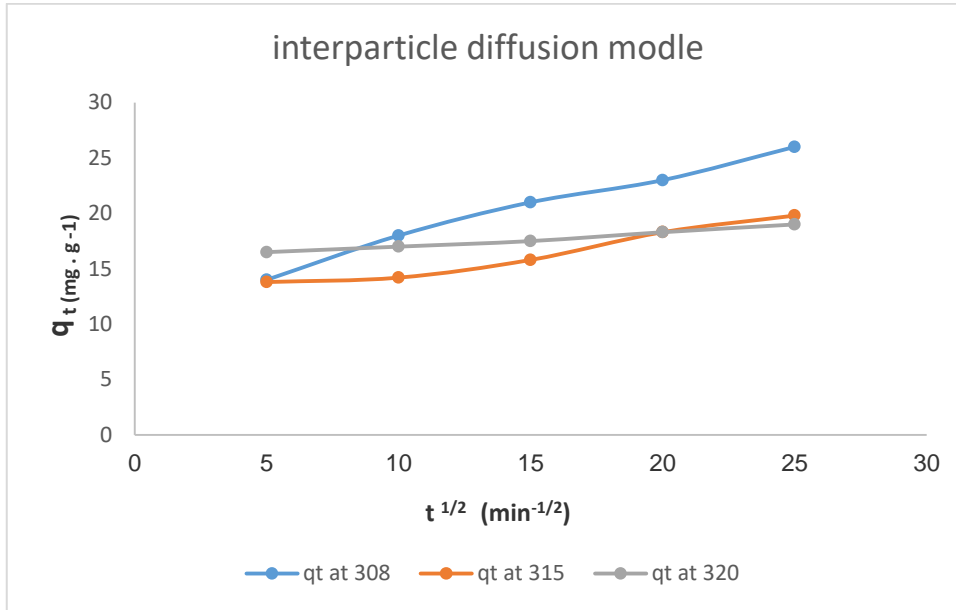


Figure 4 : Intra particle diffusion model

Table 9: Intraparticle diffusion model parameters

Intra particle diffusion model			
Temp. (K)	308	315	320
Slope K_i	0.58	0.322	0.126
Intercept C	11.7	11.55	15.77
R^2	0.9871	0.9555	0.9893

From figure 15 of the plots of q_t versus $t^{1/2}$ is almost straight which indicates an intra particle diffusion effect [64]. From the value of the intercept (C) which indicates the thickness of layer of adsorption. Larger C

values mean larger boundary effect. In the other hand when $C=0$, this means the adsorption process is controlled by intra particle diffusion.

Other fact that the linear portions of the intra particle diffusion curves did not pass through the origin, which means the adsorption process is controlled by the rate of adsorption.

4.6 Theoretical results

4.6.1 DFT study

As mentioned above, the main aim of this research study is the removal of the **TMP** from wastewater using **SiNP**. So that our discussion focuses on the results obtained in aqueous solution. The optimized geometrical structures, the molecular electrostatic potential maps (ESP) and the distribution of HOMO orbital and LUMO orbital of the **TMP** compound are shown in Figure 16 (b and c). We found that the distribution of the electron cloud in these two orbitals was mainly concentrated on the most of the entire moiety of the molecule. In particular, we found that the HOMO orbital was more distributed on the N atom and the delocalized π -electrons of the pyrimidine and the aromatic benzene ring. This finding suggests that the N atoms and the delocalized π -electrons are responsible to donate the electrons to interact with the **SiNP** surface. On the other hand, we also found that the LUMO was found more distributed on the C atoms, suggesting that the C atoms are the centers that responsible to accept electron from the **SiNP**. These findings were also confirmed by monitoring the ESP map (see Figure 16 (d)). The small value of the energy gap

indicates the high reactivity and the ease of the adsorption process of the **TMP** on the **SiNP** surface (Table 10). As is known, in the process of adsorption of **TMP** by **SiNP**, the electron charge is transferred from the **TMP** toward the **SiNP** surface, and this result is in agreement with positive values charge transfer maximum parameter (ΔN) [65]. The positive value of ΔN proves that the **TMP** has donor electron effect and is a donor electron (Table 10). Furthermore, the chemical electronic potential of the **TMP** is negative and it means that the **TMP** is stable and it is not decompose spontaneously into the elements and compounds are made up of them. The energy gap of **TMP** is quite high. The dipole moment of **TMP** (4.97 Debye) is higher than that of water (1.82 Debye) and it means that **TMP** able to expel water from the **SiNP** surface (Table 10).

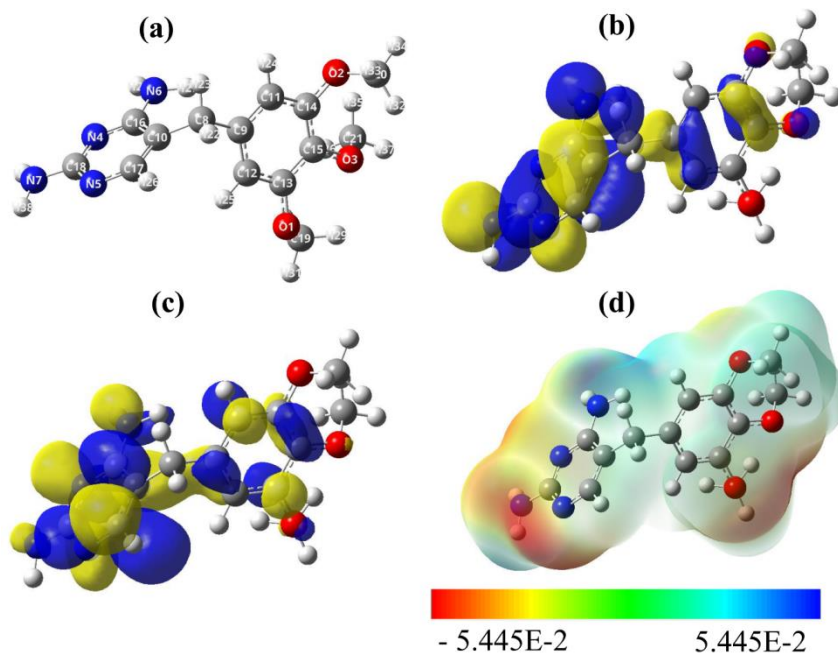


Figure 17: (a) optimized structure, (b) HOMO, (c) LUMO and (d) molecular electrostatic potential map (ESP) obtained using B3LYP/6-31+G(d,p) level of theory in gas phase.

Table 10: Quantum global reactivity descriptors of the TMP molecule

	Gas phase	aqueous solution
E_{total} (hartree)	-989.054	-989.071
Volume (bohr ³ /mol)	2174.001	2561.223
Dipole moment μ^* (Debye)	4.05	4.97
E_{HUMO} (eV)	-5.883	-6.154
E_{LUMO} (eV)	-0.637	-0.897
$E_{\text{HOMO-1}}$ (eV)	-6.346	-6.522
$E_{\text{HOMO-2}}$ (eV)	-6.590	-6.803
Energy gap ΔE (eV)	5.245	5.258
Hardness (η) (eV)	2.623	2.629
hyper-hardness (γ)	4.782	4.890
Softness S (eV ⁻¹)	0.381	0.380
Chemical potential (π) (eV)	-3.260	-3.525
Electrophilicity (ω) (eV)	2.026	2.364
Maximum charge transfer (ΔN)	1.243	1.341

Full set of the NBO charges, LRDs and DDs obtained at B3LYP/6-31+G(d,p) level of theory in aqueous solution are listed in Table S1 of the electronic supplementary information (ESI). Figure 16 (a-c) shows the graphical representation of the LRDs (f_k^\pm , σ_k^\pm and $\omega\sigma_k^\pm$, respectively) of **TMP** compound. Our computed results suggest that the highest nucleophilic attack (f_k^+) are found on C17, N4 and C16, whereas, the highest electrophilic attack (f_k^-) are found on C10, N5, N7 and N6, see (Figure S1 (a)). As known, the most nucleophilic sites in investigated compounds have the highest value of σ_k^- and ω_k^- , while the highest value of σ_k^+ and ω_k^+ reveals the most electrophilic site in **TMP** compound [66], see panels (b) and (c) of figure 16. For numerical results, see Table S1 of the ESI. Consequently,

similar conclusions can also be marked by following the results of the local softness and the local electrophilicity.

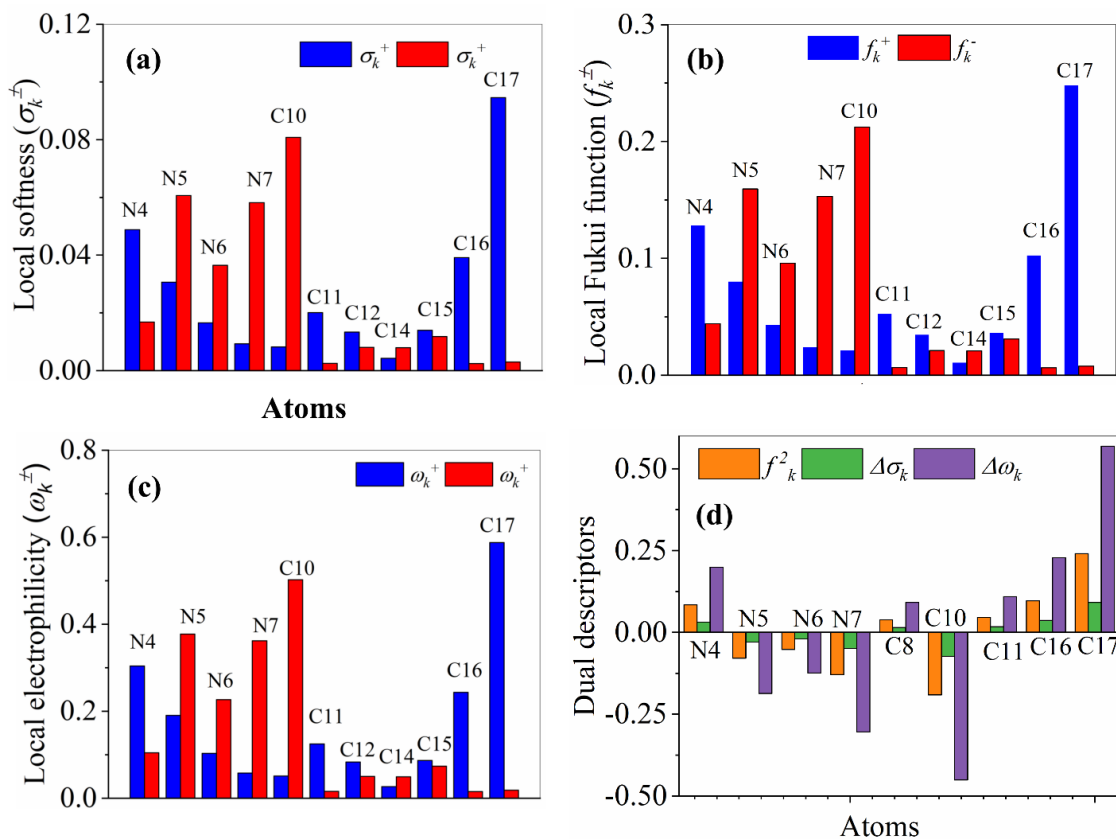


Figure 5: Graphical representation of the LRDs

(a) f_k^\pm , (b) σ_k^\pm , (c) ω_k^\pm , and (d) the local dual descriptors, (f_k^2 , $\Delta\sigma_k$ and $\Delta\omega_k$) based on Fukui Functions of the **TMP** compound obtained using B3LYP/6-31+G(d,p) level of theory in aqueous solution (the atom-numbering is in correspond with Figure 1a). (d) shows the graphical representations of the dual reactivity descriptors of **TMP** compound obtained using B3LYP/6-31+G(d,p) level of theory in aqueous solution. Full set of numerical results of the DDs can be followed in Table S1 of ESI. A close inspection of the figure and Table S1 reveals that the most active sites, with $f_k^2, \Delta\sigma_k$ and $\Delta\omega_k < 0$, that are responsible to donate electron to **SiNP** surface are C10, N7, N5 and N6, whereas the most active sites, with $f_k^2, \Delta\sigma_k$ and $\Delta\omega_k > 0$, that are

responsible to accept electron from **SiNP** surface are C17, C16 and N4. These results agree with the results obtained by HOMO, LUMO and ESP maps.

4.6.2 Monte Carlo (MC) and Molecular Dynamic (MD) simulation

The interaction between the modified silica surface and the TMP molecule was investigated using a large number of randomized Monte Carlo steps (configurations). The MD computations continue to employ the lowest energy geometry as provided by the MC. The simulation is performed under Periodic Boundary Conditions using the cell with dimensions presented in figure 18 (a). In the simulations the modified silica surface box is filled with 1 TMP and 650 water molecules. Prior to the MD stage the geometry was optimized using the Forcite module built into the Biovia software (tolerance for energy convergence of 1×10^{-5} kcal/mol; atom-based summation method for both electrostatic and van der Waals interactions with a cutoff distance of 15.5, a spline width of 1, and a 0.5 buffer. Atom-based summation method for both electrostatic and van der Waals interactions with a cutoff distance of 15.5, a s MD was done at 25°C with a 1 ns simulation duration using the Constant volume/constant temperature (NVT) canonical ensemble (using a 1fs time step)) [67-72]. The Berendsen thermostat maintains the T control. Calculations for MC and MD are performed using the Universal force field [73].

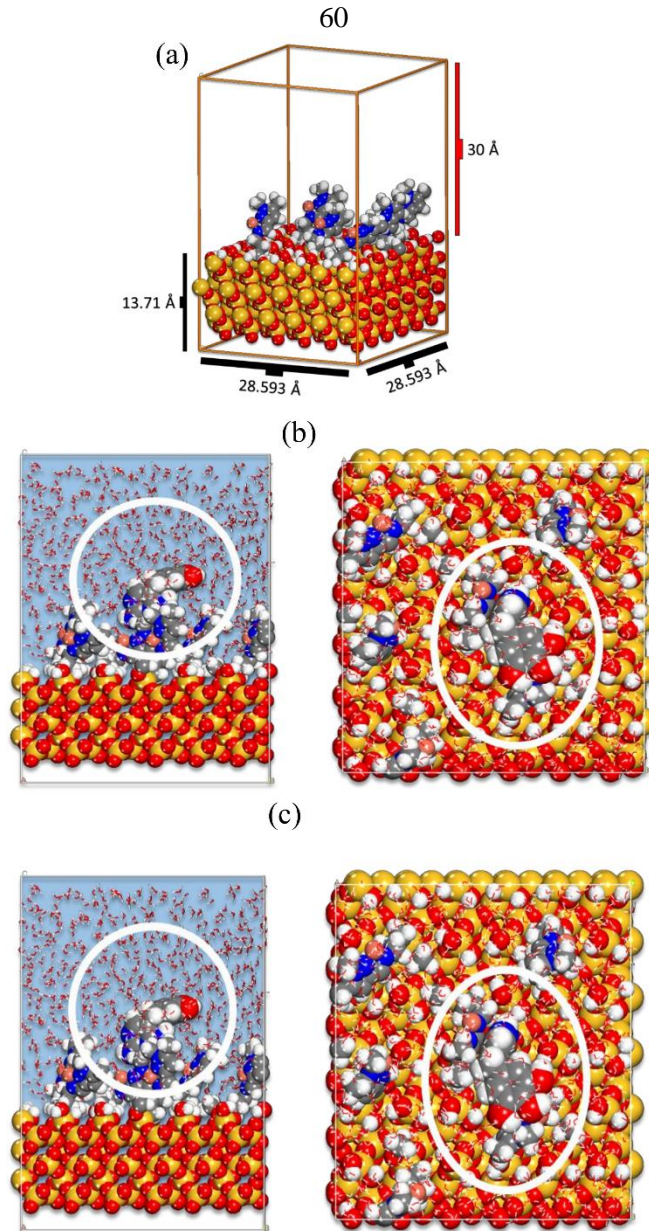


Figure 6(a) The size of the simulation box containing the modified silica surface and the vacuum layer, (b) MC pose of the lowest adsorption configurations for onto Modified silica surface and (c) Lowest energy configurations of the interaction of TMP molecule onto modified silica surface obtained by MD.

The lowest energy configurations for the silica surface and the TMP molecule are shown in Figure 18 (c). The measurable verdict of the interaction between TMP molecule and the modified silica surface is calculated using the following equation:

$$E_{ads} = E_{total} - [E_{TMP} + E_{Modified\ silica}]$$

Where: E_{total} is the total energy of the system as a result of Modified Silica surface and the TMP molecule interaction; $E_{\text{Cu(II) or Pb(II) ions}}$ and $E_{\text{Modified silica}}$ is system energy in the absence and presence of TMP molecule. MC calculations yield the lowest energy pose after a considerable number of randomized configurations. The Monte Carlo simulations (Figure 18 (b)) show that the TMP molecule adsorbs extensively on the modified silica surface, which is consistent with the experimental findings. The adsorption's negative value indicates the adsorption process' spontaneity on this adsorbent [74]. Figure S1 (a-d) , in the ESI depicts the energies during the attendance of the lowest energy position,. The distribution of the adsorption energies for the TMP molecule on the modified silica surface gained via MC, the graph of temperature control from MD during the interaction of the TMP molecule onto modified silica surface and the interaction energy of the TMP molecule onto modified silica surface during MD, respectively.

The distribution of the adsorption energies as shown in the Figure 18 (b) are in range -5 to -95 kcal/mol depending on the contact configurations among TMP and modified silica surface. MD is primarily concerned with monitoring the overall dynamics of the process [75]. The small temperature drift on the graph in Figure S3 (c) shows that the equilibrium configuration has been reached. Figure 18 (c) shows the lowest equilibrium energy structure for the TMP molecule interaction with modified silica surface obtained from MD. The interaction (adsorption) energy during the MD is assessed at each time elapse and is presented in the Figure 18 (c) and

descriptive statistics in Table 11. Relative high adsorption energies are consistent with experimental findings. The negative values of the adsorption energies indicate the spontaneity of the adsorption process.

Table 11: Statistics of the interaction energy of the TMP molecule onto modified silica surface during MD (energy values are in kcal/mol).

Molecule	Mean	Minimum	Median	Maximum
TMP	-15.48	-3.78	-16.51	-29.58

Recently, several research studies for pharmaceutical and personal care products (PPCPs) have been occurring around the world because of their severe distribution, continuous release, and huge effects on wildlife in the environment have been studied for their removal from wastewater. This study includes the use of 1,5-Dimethyl-1*H*-pyrazole-3-carbaldehyde that has been fixed on the silica surface after several treatment and modification using 3-aminopyltrimethoxysilane and refluxed with copper nitrate to end up with SiNP-Cu which was used as adsorbent for the removal of TMP. The adsorbent showed a high percentage removal towards TMP, which reached more than 94%. The new synthesized material was characterized by FT-IR spectra, nitrogen adsorption-desorption isotherm, BET surface area, B.J.H. pore sizes, thermal gravimetric analysis (TGA), and scanning electron microscopy (SEM). The new chelating surface exhibits good chemical and thermal stability. The sample was easily regenerated by soaking the sample in 6 N HCl for a few minutes (5-10 mL of 6 N HCl per g of support). The sorbent was regenerated five times. It showed no significant decrease in extraction percentage. The absorption process showed very high pH dependent and it followed Freundlich and pseudo

second order adsorption models. The adsorption process was not spontaneous.

The global reactivity indices prove that **TMP** is stable and it can be removed from wastewater using **SiNP** surface. The results of the local reactivity indices concluded that the active centers for the adsorption process are the nitrogen atoms and the π -electrons of the pyrimidine and benzene rings. Furthermore, the positive value of the maximum charge transfer number (ΔN) proves that **TMP** has a great tendency to donate electrons to **SiNP** surface during the process of adsorption.

The relative high adsorption energies obtained by MD simulation study are consistent with experimental findings. The negative values of the adsorption energies indicate the spontaneity of the adsorption process.

Conclusions

1. The results of characteristics of SiNP and their performance in **TMP** removal from aqueous solution show highly dependent on initial concentration, adsorbent dosage, the solution pH and temperature.
2. It was found that adsorption of **TMP** using (Si-NP) obeyed both Langmuir and Freundlich isotherm models, but mostly fitted with Freundlich model.
3. The adsorption capacity of (Si-NP) followed pseudo second order model, Q_e calc. (42.86, 22.23, 47.85) was in consistent with the experimental value (Q_e exp. 27.1 , 20.53 , 19.15) at three temperature studied.
4. Thermodynamic parameters of the adsorption of **TMP** on (Si-NP) revealed the following:
 - The positive ΔG° values 2.901 to 2.975 kJ/mol) indicated that the adsorption is nonspontaneous at measured temperatures.
 - The positive value of ΔH° (3.78 kJ/mol) reflected an endothermic adsorption.
 - A positive value of ΔS° (2.77 J/mol K) suggested dissociative mechanism processes.

- Si-NP matrix removed TMP from wastewater. TMP is mainly based on the chelation between the amine groups of the TMP with the metals, in order to prevent the hazardous effects of TMP in the case of disposal in the aquatic environment. SiNP is a good sorbent, which can be used for the removal of TMP from wastewater treatment plants.
- A new sorbent that facilitates chelation, and increases the adsorption capacity.

Recommendations

- Since kinetic pseudo - second order further investigation is required to study the removal mechanism of TMP.
- The possibility of using this matrix as stationary phase for HPLC.
- Studying the effect of presence of metal ions in the aqueous medium on TMP adsorption.

References

1. M. C. Bastos, M. Soubrand, T. Le Guet, É. Le Floch, E. Joussein, M. Baudu, and M. Casellas, "Occurrence, fate and environmental risk assessment of pharmaceutical compounds in soils amended with organic wastes," *Geoderma*, vol. 375, p. 114498, 2020..
2. Y. Bao, F. Li, L. Chen, Q. Mu, B. Huang, and D. Wen, "Fate of antibiotics in engineered wastewater systems and receiving water environment: A case study on the coast of Hangzhou Bay, China," *Science of the Total Environment*, vol. 769, p. 144642, 2021.
3. W.S. Chai, J.Y. Cheun, P.S. Kumar, M. Mubashir, Z. Majeed, F. Banat, & P.L. Show, " A review on conventional and novel materials towards heavy metal adsorption in wastewater treatment application", *Journal of Cleaner Production*, vol. 296, p.126589, 2021.
4. P. Chaturvedi, P. Shukla, B. S. Giri, P. Chowdhary, R. Chandra, P. Gupta, and A. Pandey, "Prevalence and hazardous impact of pharmaceutical and personal care products and antibiotics in environment: A review on emerging contaminants," *Environmental Research*, p. 110664, 2021.
5. . M. Ahmaruzzaman, & S.R. Mishra," Photocatalytic performance of g-C₃N₄ based nanocomposites for effective degradation/removal of dyes from water and wastewater", *Materials Research Bulletin*, vol.143, P. 111417, 2021.

6. F. Wollmann, S. Dietze, S.,J.U. Ackermann, T. Bley, T. Walther, J. Steingroewer, & F. Krujatz, "Microalgae wastewater treatment: biological and technological approaches", *Engineering in Life Sciences*, vol. 19(12), 860-871, 2019.
7. C. Su, Y. Cui, D. Liu, H. Zhang, &Y. Baninla, , "Endocrine disrupting compounds, pharmaceuticals and personal care products in the aquatic environment of China: Which chemicals are the prioritized ones? ", *Science of The Total Environment*, vol. 720, p. 137652, 2020.
8. L. Yao, Y. Wang, L. Tong, Y. Deng, Y. Li, ,Y. Gan , & K. Zhao, "Occurrence and risk assessment of antibiotics in surface water and groundwater from different depths of aquifers: A case study at Jiangnan Plain, central China ", *Ecotoxicology and Environmental Safety*, vol.135, pp. 236-242, 2017.
9. J. Cheng, X. Tang, & C. Liu, "Occurrence and distribution of antibiotic resistance genes in various rural environmental media", *Environmental Science and Pollution Research*, vol.27, pp.29191-29203, 2020.
10. L. Nielsen, & T.G. Badosz, "Analysis of sulfamethoxazole and trimethoprim adsorption on sewage sludge and fish waste derived adsorbents", *Microporous and Mesoporous Materials*, vol. 220, pp 58-72, 2016.

11. X. Bai, & K. Acharya, "Removal of trimethoprim, sulfamethoxazole, and triclosan by the green alga *Nannochloris* sp.," *Journal of hazardous materials*, vol. 315, pp. 70-75, 2016.
12. T. Thibaut, "Sulfamethoxazole/Trimethoprim ratio as a new marker in raw wastewaters: A critical review", *Science of the Total Environment*, vol. 715, p 136916, 2020.
13. S. Wang, & J. Wang, "Trimethoprim degradation by Fenton and Fe (II)-activated persulfate processes. *Chemosphere*, vol. 191, pp. 97-105, 2018.
14. V. Sharma, R.V. Kumar, K. Pakshirajan, & G. Pugazhenti, "Integrated adsorption-membrane filtration process for antibiotic removal from aqueous solution", *Powder technology*, vol. 321, pp. 259-269, 2017.
15. L. Gurreri, A. Tamburini, A. Cipollina, & G. Micale, "Electrodialysis applications in wastewater treatment for environmental protection and resources recovery: A systematic review on progress and perspectives", *Membranes*, vol. 10(7), p. 146, 2020.
16. D. Ghernaou, & N. Elboughdiri, "Advanced oxidation processes for wastewater treatment: facts and future trends", *Open Access Library Journal*, vol. 7(2), p. 1-15, 2020.
17. C. Wei, F. Zhang, Y. Hu, C. Feng, & H. Wu, "Ozonation in water treatment: the generation, basic properties of ozone and its practical

- application", *Reviews in Chemical Engineering*, vol. 33(1), p.49-89, 2017.
18. I. Levchuk , J.J.R. Márquez, & M. Sillanpää, " Removal of natural organic matter (NOM) from water by ion exchange—a review", *Chemosphere*, vol. 192, p.90-104, 2018.
 19. B.P. Chaplin, "The prospect of electrochemical technologies advancing worldwide water treatment", *Accounts of chemical research*, vol. 52(3), p.596-604, 2019.
 20. L. Lan , X. Kong , H . Hi. C. Sun, &D. Liu, "High removal efficiency of antibiotic resistance genes in swine wastewater via nanofiltration and reverse osmosis processes", *Journal of environmental management*, vol.231, p.439-445, 2019.
 21. A. Saravanan , P.S. Kumar, S. Jeevanantham ,S. Karishma, B. Tajsabreen, , P.R. Yaashikaa & B. Reshma, " Effective water/wastewater treatment methodologies for toxic pollutants removal: Processes and applications towards sustainable development". *Chemosphere*, vol. 280, 130595, 2021.
 22. L.F. Angeles, R.A. Mullen ,I.J. Huang, C. Wilson, W. Khunjar, H.I. Sirotkin & D.S. Aga , "Assessing pharmaceutical removal and reduction in toxicity provided by advanced wastewater treatment systems". *Environmental Science: Water Research & Technology*, vol.6 (1), p. 62-77, 2020.

23. N. Nouri, P. Khorram, O. Duman, T. Sibel, & S. Hassan, "Overview of nanosorbents used in solid phase extraction techniques for the monitoring of emerging organic contaminants in water and wastewater samples". *Trends in Environmental Analytical Chemistry*, vol.25, e0008, 2020.
24. E.F. Vansant, P. Van Der Voort, & K.C. Vrancken, "Characterization and chemical modification of the silica surface". *Elsevier*, vol.93, 1995.
25. S. Radi, S. Tighadouini, M. Bacquet, S. Degoutin, F. Cazier, M. Zaghrioui, and Y. N. Mabkhot, "Organically modified silica with pyrazole-3-carbaldehyde as a new sorbent for solid-liquid extraction of heavy metals," *Molecules*, vol. 19, pp. 247-262, 2014.
26. Y. Toubi, S. Radi, and M. Bacquet, "Synthesis of pyridin-3-yl-functionalized silica as a chelating sorbent for solid-phase adsorption of Hg (II), Pb (II), Zn (II), and Cd (II) from water," *Research on Chemical Intermediates*, vol. 39, pp. 3791-3802, 2013..
27. P. E. N. T. T. I. Huovinen, "Trimethoprim resistance". *Antimicrobial agents and chemotherapy*, vol. 31(10), p.1451-1456, 1987.
28. J. Mazurek-Popczyk & K. Baldy-Chudzik, "Differentiation of Trimethoprim Resistance Genes among Escherichia coli Strains from an Environment with Intensive Supply of Antibiotics", *sci. form*, 2021.

29. M.E. Ali, Hoque, S.K. Safdar Hossain, & M.C. Biswas, " Nanoadsorbents for wastewater treatment: next generation biotechnological solution". *International Journal of Environmental Science and Technology*, vol. 17, p. 4095-4132, 2020.
30. H.B.Quesada, A.T.A. Baptista, L.F. Cusioli , D. Seibert, "de Oliveira Bezerra, C., & Bergamasco, R. Surface water pollution by pharmaceuticals and an alternative of removal by low-cost adsorbents: A review". *Chemosphere*, vol. 222, p. 766-780, 2019.
31. S.D. Faust, & O.M. Aly, "Adsorption processes for water treatment". *Elsevier*, vol. 29, 2013.
32. N. Abd-Talib , S.H. Mohd-Setapar, &A.K. Khamis , "The benefits and limitations of methods development in solid phase extraction: Mini review", *Jurnal Teknologi*, vol. 69(4).2014
33. J. Feitosa-Felizzola, B. Temime, and S. Chiron, "Evaluating on-line solid-phase extraction coupled to liquid chromatography–ion trap mass spectrometry for reliable quantification and confirmation of several classes of antibiotics in urban wastewaters," *Journal of Chromatography A*, vol. 1164, pp. 95-104, 2007.
34. S. Asgari, H. Bagheri, and A. Es-Haghi, "Super-porous semi-interpenetrating polymeric composite prepared in straw for micro solid phase extraction of antibiotics from honey, urine and

- wastewater," *Journal of Chromatography A*, vol. 1631, p. 461576, 2020.
35. A. Sarkar, P. Datta, and M. Sarkar, "Sorption recovery of metal ions using silica gel modified with salicylaldehyde," *Talanta*, vol. 43, pp. 1857-1862, 1996.
 36. P. M. Price, J. H. Clark, and D. J. Macquarrie, "Modified silicas for clean technology," *Journal of the Chemical Society, Dalton Transactions*, pp. 101-110, 2000.
 37. G. Grigoropoulou, P. Stathi, M. Karakassides, M. Louloudi, and Y. Deligiannakis, "Functionalized SiO₂ with N-, S-containing ligands for Pb (II) and Cd (II) adsorption," *Colloids and Surfaces A: Physicochemical and Engineering Aspects*, vol. 320, pp. 25-35, 2008.
 38. X. Chen, "Modeling of experimental adsorption isotherm data". *Information* vol. 6(1), p.14-22, 2015.
 39. E.N. El Qada , S.J. Allen, & G.M. Walker. "Adsorption of methylene blue onto activated carbon produced from steam activated bituminous coal: a study of equilibrium adsorption isotherm". *Chemical Engineering Journal*, vol. 124(1-3), p.103-110, 2006.
 40. T.S. Khayyun, &A.H. Mseer, "Comparison of the experimental results with the Langmuir and Freundlich models for copper removal on limestone adsorbent". *Applied Water Science*, vol. 9(8), 1-8, 2019.

41. E. C. Lima, F. Sher, A. Guleria, M.R.Saeb, I. Anastopoulos , H.N. Tran & A. Hosseini-Bandegharai . "Is one performing the treatment data of adsorption kinetics correctly?" *Journal of Environmental Chemical Engineering*, vol. 9(2), 104813, 2021.
42. E.C. Lima, A.A. Gomes ,& H.N. Tran, " Comparison of the nonlinear and linear forms of the van't Hoff equation for calculation of adsorption thermodynamic parameters (ΔS° and ΔH°)". *Journal of Molecular Liquids*, vol.311, 113315, 2020.
43. Y. Uppa, T. Taweetanavanich, C. Kaewtong &N. Niamsa, "Immobilization of unmodified aminoanthraquinone derivatives onto silica gel surface for solid-phase extraction and pre-concentration of Pb (II) ". *Environmental technology*, vol. 42(8), p.1252-1259, 2021.
44. Y. Toubi, S. Radi, and M. Bacquet, "Synthesis of pyridin-3-yl-functionalized silica as a chelating sorbent for solid-phase adsorption of Hg (II), Pb (II), Zn (II), and Cd (II) from water," *Research on Chemical Intermediates*, vol. 39, pp. 3791-3802, 2013
45. S. Radi, S. Tighadouini, M. Bacquet, S. Degoutin, F. Cazier, M. Zaghrioui, and Y. N. Mabkhot, "Organically modified silica with pyrazole-3-carbaldehyde as a new sorbent for solid-liquid extraction of heavy metals," *Molecules*, vol. 19, pp. 247-262, 2014.
46. A. Frisch, "Gaussian 09w reference," *Wallingford, USA*, 25p, 2009

47. A. D. Becke, "A new mixing of Hartree–Fock and local density-functional theories," *The Journal of chemical physics*, vol. 98, pp. 1372-1377, 1993.
48. R. Parr and W. Yang, "Density-functional theory of atoms and molecules Oxford Univ. Press," *ed: Oxford*, 1989.
49. C. Lee, W. Yang, and R. G. Parr, "Development of the Colle-Salvetti correlation-energy formula into a functional of the electron density," *Physical review B*, vol. 37, p. 785, 1988.
50. K. B. Wiberg, "Ab Initio Molecular Orbital Theory by WJ Hehre, L. Radom, P. v. R. Schleyer, and JA Pople, John Wiley, New York, 548pp. Price: \$79.95 (1986)," *ed: Wiley Online Library*, 1986.
51. B. Mennucci, J. Tomasi, R. Cammi, J. Cheeseman, M. Frisch, F. Devlin, S. Gabriel, and P. Stephens, "Polarizable continuum model (PCM) calculations of solvent effects on optical rotations of chiral molecules," *The Journal of Physical Chemistry A*, vol. 106, pp. 6102-6113, 2002.
52. S. Miertuš, E. Scrocco, and J. Tomasi, "Electrostatic interaction of a solute with a continuum. A direct utilizaion of AB initio molecular potentials for the prevision of solvent effects," *Chemical Physics*, vol. 55, pp. 117-129, 1981.
53. R. Cammi and J. Tomasi, "Remarks on the use of the apparent surface charges (ASC) methods in solvation problems: Iterative versus matrix-inversion procedures and the renormalization of the

- apparent charges," *Journal of computational chemistry*, vol. 16, pp. 1449-1458, 1995.
54. Ş. Erdoğan, Z. S. Safi, S. Kaya, D. Ö. Işın, L. Guo, and C. Kaya, "A computational study on corrosion inhibition performances of novel quinoline derivatives against the corrosion of iron," *Journal of Molecular Structure*, vol. 1134, pp. 751-761, 2017.
55. L. Guo, Z. S. Safi, S. Kaya, W. Shi, B. Tüzün, N. Altunay, and C. Kaya, "Anticorrosive effects of some thiophene derivatives against the corrosion of iron: a computational study," *Frontiers in chemistry*, vol. 6, p. 155, 2018.
56. W. Yang and W. J. Mortier, "The use of global and local molecular parameters for the analysis of the gas-phase basicity of amines," *Journal of the American Chemical Society*, vol. 108, pp. 5708-5711, 1986.
57. K. Fukui, "Role of frontier orbitals in chemical reactions," *Science*, vol. 218, pp. 747-754, 1982.
58. C. Lee, W. Yang, and R. G. Parr, "Local softness and chemical reactivity in the molecules CO, SCN⁻ and H₂CO," *Journal of Molecular Structure: THEOCHEM*, vol. 163, pp. 305-313, 1988.
59. J. I. Martínez-Araya, "Why is the dual descriptor a more accurate local reactivity descriptor than Fukui functions?" *Journal of Mathematical Chemistry*, vol. 53, pp. 451-465, 2015.

60. C. Cárdenas, N. Rabi, P. W. Ayers, C. Morell, P. Jaramillo, and P. Fuentealba, "Chemical reactivity descriptors for ambiphilic reagents: dual descriptor, local hypersoftness, and electrostatic potential," *The Journal of Physical Chemistry A*, vol. 113, pp. 8660-8667, 2009.
61. O. Dagdag, Z. Safi, N. Wazzan, H. Erramli, L. Guo, A. M. Mkadmh, C. Verma, E. Ebenso, L. El Gana, and A. El Harfi, "Highly functionalized epoxy macromolecule as an anti-corrosive material for carbon steel: Computational (DFT, MDS), surface (SEM-EDS) and electrochemical (OCP, PDP, EIS) studies," *Journal of Molecular Liquids*, vol. 302, p. 112535, 2020.
62. S. Jodeh, F. Abdelwahab, N. Jaradat, I. Warad, and W. Jodeh, "Adsorption of diclofenac from aqueous solution using Cyclamen persicum tubers based activated carbon (CTAC)," *Journal of the Association of Arab Universities for Basic and Applied Sciences*, vol. 20, pp. 32-38, 2016.
63. B. Khalaf, O. Hamed, S. Jodeh, G. Hanbali, R. Bol, O. Dagdag, and S. Samhan, "Novel, Environment-Friendly Cellulose-Based Derivatives for Tetraconazole Removal from Aqueous Solution," *Polymers*, vol. 13, p. 450, 2021.
64. S. Jodeh, O. Hamed, A. Melhem, R. Salghi, D. Jodeh, K. Azzaoui, Y. Benmassaoud, and K. Murtada, "Magnetic nanocellulose from olive industry solid waste for the effective removal of methylene

- blue from wastewater," *Environmental Science and Pollution Research*, vol. 25, pp. 22060-22074, 2018.
65. M. Rezaei-Sameti and P. Zarei, "NBO, AIM, HOMO–LUMO and thermodynamic investigation of the nitrate ion adsorption on the surface of pristine, Al and Ga doped BNNTs: A DFT study," *Adsorption*, vol. 24, pp. 757-767, 2018.
66. S. Pathak, R. Srivastava, A. Sachan, O. Prasad, L. Sinha, A. Asiri, and M. Karabacak, "Experimental (FT-IR, FT-Raman, UV and NMR) and quantum chemical studies on molecular structure, spectroscopic analysis, NLO, NBO and reactivity descriptors of 3, 5-Difluoroaniline," *Spectrochimica Acta Part A: Molecular and Biomolecular Spectroscopy*, vol. 135, pp. 283-295, 2015.
67. V. Thaçi, R. Hoti, A. Berisha, and J. Bogdanov, "Corrosion study of copper in aqueous sulfuric acid solution in the presence of (2E, 5E)-2, 5-dibenzylidenecyclopentanone and (2E, 5E)-bis [(4-dimethylamino) benzylidene] cyclopentanone: Experimental and theoretical study," *Open Chemistry*, vol. 18, pp. 1412-1420, 2020.
68. R. Hsissou, F. Benhiba, S. About, O. Dagdag, S. Benkhaya, A. Berisha, H. Erramli, and A. Elharfi, "Trifunctional epoxy polymer as corrosion inhibition material for carbon steel in 1.0 M HCl: MD simulations, DFT and complexation computations," *Inorganic Chemistry Communications*, vol. 115, p. 107858, 2020.

69. R. Hsissou, S. About, R. Seghiri, M. Rehioui, A. Berisha, H. Erramli, M. Assouag, and A. Elharfi, "Evaluation of corrosion inhibition performance of phosphorus polymer for carbon steel in [1 M] HCl: Computational studies (DFT, MC and MD simulations)," *Journal of Materials Research and Technology*, vol. 9, pp. 2691-2703, 2020.
70. R. Hsissou, O. Dagdag, S. About, F. Benhiba, M. Berradi, M. El Bouchti, A. Berisha, N. Hajjaji, and A. Elharfi, "Novel derivative epoxy resin TGETET as a corrosion inhibition of E24 carbon steel in 1.0 M HCl solution. Experimental and computational (DFT and MD simulations) methods," *Journal of Molecular Liquids*, vol. 284, pp. 182-192, 2019.
71. O. Dagdag, A. Berisha, Z. Safi, O. Hamed, S. Jodeh, C. Verma, E. Ebenso, and A. El Harfi, "DGEBA-polyaminoamide as effective anti-corrosive material for 15CDV6 steel in NaCl medium: Computational and experimental studies," *Journal of Applied Polymer Science*, vol. 137, p. 48402, 2020.
72. O. Dagdag, R. Hsissou, A. El Harfi, A. Berisha, Z. Safi, C. Verma, E. Ebenso, M. E. Touhami, and M. El Gouri, "Fabrication of polymer based epoxy resin as effective anti-corrosive coating for steel: Computational modeling reinforced experimental studies," *Surfaces and Interfaces*, vol. 18, p. 100454, 2020.

73. A. K. Rappé, C. J. Casewit, K. Colwell, W. A. Goddard III, and W. M. Skiff, "UFF, a full periodic table force field for molecular mechanics and molecular dynamics simulations," *Journal of the American Chemical Society*, vol. 114, pp. 10024-10035, 1992.
74. V. V. Mehmeti and A. R. Berisha, "Corrosion study of mild steel in aqueous sulfuric acid solution using 4-methyl-4H-1, 2, 4-Triazole-3-Thiol and 2-mercaptonicotinic acid—an experimental and theoretical study," *Frontiers in chemistry*, vol. 5, p. 61, 2017.
75. O. Amrhar, A. Berisha, L. El Gana, H. Nassali, and M. S. Elyoubi, "Removal of methylene blue dye by adsorption onto Natural Muscovite Clay: experimental, theoretical and computational investigation," *International Journal of Environmental Analytical Chemistry*, pp. 1-26, 2021.
76. Z. B. Molu and K. Yurdakoç, "Preparation and characterization of aluminum pillared K10 and KSF for adsorption of trimethoprim," *Microporous and Mesoporous Materials*, vol. 127, pp. 50-60, 2010.
77. F. Mehrabi, M. Mohamadi, A. Mostafavi, H. Hakimi, & T. Shamspur, " Magnetic solid phase extraction based on PVA-TEOS/grafted Fe₃O₄@ SiO₂ magnetic nanofibers for analysis of sulfamethoxazole and trimethoprim in water samples, " *Journal of Solid State Chemistry*", vol.292, p.121716, 2020..
78. Q. Liu, M. Li, X. Liu, Q. Zhang, R. Liu, Z. Wang, & F. Zhang, "Removal of sulfamethoxazole and trimethoprim from reclaimed

- water and the biodegradation mechanism", *Frontiers of environmental science & engineering*, vol. 12(6) , P. 1-8, 2018.
79. D. Mansour, F. Fourcade, I. Soutrel, D. Hauchard, N. Bellakhal, & A. Amrane, " Mineralization of synthetic and industrial pharmaceutical effluent containing trimethoprim by combining electro-Fenton and activated sludge treatment", *Journal of the Taiwan institute of chemical engineers*, vol.53,p. 58-67, 2015.
80. M.Samy, M.G. Ibrahim, M.G. Alalm, M. Fujii , S. Ookawara , & T. Ohno, " Photocatalytic degradation of trimethoprim using S-TiO₂ and Ru/WO₃/ZrO₂ immobilized on reusable fixed plates". *Journal of Water Process Engineering*, vol.33, p.101023, 2020.

Appendix's

Data of experiment 1: Effect of contact time

Contact time (min)	q _e 308K	q _e 315K	q _e 320K
0	5	6	7
10	7	9	11
20	13	13.6	13.8
50	14	15	16
90	19	19.5	19.9
100	21	21.7	22.1
150	22	23	23.5

Temperature = 25 C°

Concentration of TMP = 10 mg/L

Solution volume= 50 mL

Adsorbent dose= 0.03 g

Data of experiment 2: Effect of pH

pH	Adsorption %
2	35
4	53
6	67
8	87
10	89
12	92

C_o= 10 ppm

Temperature= 25 C°

Time= 100 min.

Adsorbent dose=0.03g

Solution volume=50mL

Data of experiment 3: Effect of temperature

Temp. (k)	K_c	$\ln K_c$	$1/T$ ($k^{-1} * 10^{-3}$)	ΔH^0 K j/mol	ΔS^0 j/mol k	ΔG^0 K j/mol k
308	0.318	-1.1457	3.785	3.566	2.7718	2.934
315	0.321	-1.13631	3.175	3.566	2.7718	2.976
320	0.336	-1.09064	3.125	3.566	2.7718	2.902

p H= 8

Time = 100 min.

Adsorbent dose= 0.03g,

Solution volume= 50 mL

Data of experiment 5: Effect of amount of adsorbent

Weight of dose(g)	C_s
0.01	3.7
0.03	4.1
0.08	4.4
0.1	5.6
0.2	6.8
0.3	8.2

Temperature=25 °C

Time= 100 min.

P H= 8

Concentration of TMP =10 mg/L

Solution volume= 50 mL

Adsorption isotherm of TMP

C_e	Cs at 308	Cs at 315	Cs at 320	Ce/Cs at 308	Ce/Cs at 315	Ce/Cs at 320
0	0.003	0.008	0.01	0	-	-
0.02	0.009	0.012	0.02	2.2222	1.6666	1
0.03	0.01	0.021	0.03	3	1.4285	1
0.04	0.022	0.032	0.04	1.81818	1.25	1
0.05	0.03	0.041	0.05	1.6666	1.2195	1
0.06	0.041	0.052	0.061	1.4634	1.1538	0.9836
0.07	0.058	0.068	0.072	1.2068	1.0294	0.9722
0.08	0.062	0.082	0.095	1.2903	0.9756	0.8421
0.09	0.073	0.098	0.12	1.2328	0.91836	0.75
0.1	0.09	0.11	0.14	1.1111	0.9090	0.7142

$\ln C_e$	$\ln C_s$ at 308	$\ln C_s$ at 315	$\ln C_s$ at 320
	-5.80914	-4.82831	-4.60517
-3.91202	-4.71053	-4.42285	-3.91202
-3.50656	-4.60517	-3.86323	-3.50656
-3.21888	-3.81671	-3.44202	-3.21888
-2.99573	-3.50656	-3.19418	-2.99573
-2.81341	-3.19418	-2.95651	-2.79688
-2.65926	-2.84731	-2.68825	-2.63109
-2.52573	-2.78062	-2.50104	-2.35388
-2.40795	-2.6173	-2.32279	-2.12026
-2.30259	-2.40795	-2.20727	-1.96611

Adsorption kinetics of TMP

$t^{1/2}$	Time (min)	Q_t at 308C	Q_t at 315C	Q_t at 320C	1/time	$1/Q_t$ at 308C	$1/Q_t$ at 315C	$1/Q_t$ at 320C
5	25	14	13.8	16.5	0.04	0.071429	0.07246	0.0606
10	100	18	14.2	17	0.01	0.05555	0.07042	0.0588
15	225	21	15.8	17.5	0.00444	0.047619	0.0632	0.05714
20	400	23	18.3	18.3	0.0025	0.043478	0.05464	0.05464
25	625	26	19.8	19	0.0016	0.03846	0.0505	0.0526

$$Q_e = 2.783$$

جامعة النجاح الوطنية

كلية الدراسات العليا

إزالة ثلاثي ميثوبريم من المياه العادمة باستخدام السيلكيا المعدلة عضوياً
بالبيرازول -3 كاربالديهد المرتبط مع ايونات النحاس: المنهج التجريبي
والنظري

اعداد

الهام "محمد سعيد" داود الشيخ

بإشراف الدكتور

أ. د. شحدة جودة

قدمت هذه الأطروحة استكمالاً لمتطلبات الحصول على درجة الماجستير في الكيمياء من كلية الدراسات العليا في جامعة النجاح الوطنية، نابلس - فلسطين.

2021

ب

إزالة ثلاثي ميثوبيريم من المياه العادمة باستخدام السيليكيا المعدلة عضوياً بالبيريلازول -3

كاربالديهد المرتبط مع ايونات النحاس: المنهج التجريبي والنظري

اعداد

الهام "محمد سعيد" داود الشيخ

إشراف

أ. د شحدة جودة

المخلص

أصبحت مياه الصرف الصحي في الآونة الأخيرة مصدر قلق بسبب سمية محددة والتلوث البيئي. تشكل المضادات الحيوية خطراً على صحة الإنسان. التراييميثوبيريم هو أحد المضادات الحيوية الموجودة في مياه الصرف الصحي والقضية الرئيسية هنا هي محاولة إزالته عن طريق الامتزاز.

سوف نستخدم المادة المركبة من السليكا جل المنشط مع 3-aminopropyltrimethoxysilane بعد التحضير لتشكيل مادة ماصة معدلة جديدة من SiNP. تم تحضير المادة الماصة المربوطة الجديدة لكننا نعمل على تفاعلها مع أيونات النحاس وسنستخدم هذه المادة المعدلة كمادة مازة جديدة لإزالة التراييميثوبيريم من مياه الصرف الصحي.

يظهر السطح المعدل ثباتاً حرارياً جيداً يحدده TGA. أكدت نتائج FTIR و UV ان وحدات 1.5-dimethyl-Hpyrazole-3-carbaldehyde قد تم تثبيتها على سطح هلام السليكا المعدل.

كما أظهرت صور المسح الإلكتروني (SEM) أن السطح المعدل الجديد يتميز بطبيعة صلبة ومسامية. مما يشير الى ان المواد تقدم خصائص جيدة لاستخدامها كمادة مازة. تم فحص SiNP المعدلة كمادة مازة لإزالة التراييميثوبيريم.

أجريت تجارب الامتزاز لمجموعة واسعة من درجة الحموضة لمحاليل مختلفة، كمية المادة المازة بأوزان مختلفة ودرجة الحرارة والتركيز الابتدائي للمحاليل ومدة الاتصال. أظهرت النتائج أن النسبة المئوية لإزالة التراييميثوبيريم تزداد مع زيادة العوامل المذكورة تحققت الكفاءة العالية لإزالة

الترايبيثوبريم بعد 100 دقيقة وعند درجة حموضة حوالي 8 ،درجة حرارة 25 درجة مئوية و 0.03 غرام من وزن المادة المازة وتركيز ابتدائي الترايبيثوبريم 10 ملغم/لتر.

قيم Q_e المحسوبة 42.86، 47.85، 22.23 التي تم الحصول عليها من تفاعلات الامتزاز من الدرجة الثانية قد توافقت مع قيمة Q_e التجريبية (20.46 ، 20.38 ، 19.32) على درجات الحرارة 320K ، 315 ، 308 على التوالي . كما أن قيم R^2 كانت قريبة من 1 ، وهذا يؤكد أن عملية الامتزاز للتفاعلات من الدرجة الثانية pseudo second order mode .

كما أن قيمة $n=(1.3817 \text{ to } 1.1902)$ التي تم حسابه من نموذج Freundlich على درجات حرارة مختلفة تؤكد ان امتزاز TMP باستخدام (Si-NP) مناسبة، تم دراسة بيانات الامتزاز وفقاً لنموذج Langmuir و Freundlich ولكن نموذج Freundlich هو مناسباً أكثر لبيانات الامتزاز التجريبية . نموذج Freundlich يقترح الامتزاز الفيزيائي فضلاً عن التوزيع غير متجانس من المواقع المفعلة على سطح المازة.

قيم ΔG° الموجبة 2.933 to 2.901kJ/mol تشير إلى أن عملية الامتزاز مفضله و غير تلقائية على درجات الحرارة المذكورة. كما أن القيمة الموجبة لـ ΔH° (3.785kJ/mol) تشير إلى أن عملية الامتزاز ماصة للحرارة، وتشير الى ان عملية الامتزاز مفضلة على درجات الحرارة المذكورة. القيمة الموجبة لـ ΔS° (2.7718J/mol/K) تعكس أنها عملية ترابطيه وتعكس وجود تغيير كبير يحدث في الهياكل الداخلية للمازة أثناء عملية الامتزاز.

(Si-NP) قدمت وسيلة عملية لعلاج فعال لمياه الصرف الصحي الملوثة بالمضاد الحيوي الترايبيثوبريم.